Comparing the Euro 2k reconstruction to a regional climate model simulation

Oliver Bothe, ol.bothe@gmail.com
Helmholtz Zentrum Geesthacht, Institute of Coastal Research
Geesthacht, Germany

Abstract

We do not expect simulations and reconstructions of past climate change to agree on the exact evolution of past climate variations. Simulations with sophisticated climate models present spatially discrete but complete estimates, which are consistent relative to the implemented physics and their uncertain forcing data. Reconstruction methods statistically infer past changes from natural archives who reacted to and recorded more than one external influence and, thus, carry an uncertainty by construction. However, comparison of both data sources is relevant not least as it addresses the disagreements between the data. This manuscript describes the disagreement of a regional simulation with an ensemble of regional reconstructions but also highlights some agreement. The results emphasize the congruence in modelling and reconstructing past changes. Besides the expected disagreement both sources of information about past climate changes show some potential agreement in low frequency variability, time-series properties, and spatial covariability. While we cannot aim for perfect matches we can consider simulations and reconstructions as estimates of probabilities of past changes if their general properties agree.

1 Preliminaries

Two sources provide us with information about past climates, simulations with sophisticated models of the climate- or earth-system and reconstructions based on environmental or documentary observations from past periods (PAGES 2k-PMIP3 group, 2015). Inferrences about past climates from these proxy-observations are uncertain not least since more than one environmental factor influences the recording of the sensor (Evans et al., 2013). The simulation results are uncertain not least since we do not know the exact past boundary conditions (Schmidt et al., 2011).

Even if we knew the major forcing conditions and had the perfect proxy, internal variability on various time-scales would likely result in distinct trajectories in simulation and reconstruction (Deser et al., 2012). Furthermore, proxies, reconstructions and simulations represent different spatial scales (e.g., PAGES Hydro2k Consortium, 2017). Proxies likely record local signals, from which we may make regionalized inferrences. Simulations provide spatially discrete grids with grid-point-representative time-series. Regional models (Ludwig et al., 2018) and proxy-forward-model approaches (Evans et al., 2013; Tolwinski-Ward et al., 2011) as well as data assimilation techniques (e.g., Hakim et al., 2016) provide means for bridging the gap between the local proxies and the larger scale simulations.

Exact agreement between simulations and reconstructions is more than unlikely. Comparisons of both data sources can result in consilience of the two distinct lines of evidence about past climate evolutions (PAGES 2k-PMIP3 group, 2015). Even disagreement between both data sources is valuable as it highlights future research directions to increase our understanding of past changes.

This report compares the Euro 2k summer surface air temperature reconstruction ensemble of Luterbacher et al. (2016) and a regional climate simulation (Wagner, personal communication; PRIME2, 2018; Gómez-Navarro et al., 2015; Bierstedt et al., 2016) with the regional climate model CCLM (Rockel et al., 2008). I follow the suggested methods of the PAGES 2k-PMIP3 group (2015) but add additional analyses on time-series properties. I exclude methods for detecting forcing influences. This report is in principle another supplement to the analyses of Luterbacher et al. (2016).

To my knowledge, there has not been an effort using regional climate simulations comparable to the work by the PAGES 2k-PMIP3 group (2015) who used multiple methods to compare global simulations and continental reconstructions. Obviously, this is not least because of a lack of long transient regional climate simulations over the recent centuries except for, e.g., those used by Gómez-Navarro et al. (2013, see also Gómez-Navarro et al., 2015) and Gómez-Navarro et al. (2015, Wagner, personal communication, see also Bierstedt et al., 2016).

The current approach differs from that of the PAGES 2k-PMIP3 group (2015) not only by using a single regional climate simulation instead of an ensemble of global simulations. The availability of an ensemble for the Euro 2k reconstruction provides a range of results for the chosen analyses, which by construction gives an uncertainty measure for the comparison of reconstructions and simulations.

The next section shortly discusses the data sets and gives a short comment on the chosen approach. Afterwards I present the results for the various analyses and end with a short summary discussing these results.

2 Data and Comment on Approach

2.1 Reconstruction Data

Luterbacher et al. (2016) present two reconstructions of European summer temperature for the Common Era (CE) of the last two thousand years, the Euro 2k reconstrutions. These are an index-reconstruction and a reconstruction of spatial fields. The latter stems from an application of a Bayesian Hierarchical Modelling algorithm (BHM, compare Luterbacher et al., 2016, and their references). Their manuscript and their supplementary materials provide various comparisons of the reconstructions with the PMIP3-ensemble of global climate simulations (Schmidt et al., 2011) and other regional and local reconstructions. Luterbacher et al. (2016) select 9 sources of information for their reconstruction. These are three proxies from Scandinavia, two from the Alps, one each from Romania, Spain, and France. Additionally, the reconstruction uses a Central European area average reconstruction by Dobrovolný et al. (2016), which, in turn, considered historical documents from Central Europe. Thus, there is an obvious gap in proxy-coverage over the south-east of Europe. This in combination with the reconstruction procedure (compare Luterbacher et al., 2016) implies that one has to be especially cautious in interpreting the reconstruction there.

The BHM-reconstruction method produces an ensemble of reconstructions. This ensemble has 1000 members, which I use here. I am going to refer to the ensemble data by the abbreviation BHM.

2.2 Simulation Data

Wagner (Wagner, personal communication; PRIME2, 2018; see also Gómez-Navarro et al., 2015; Bierstedt et al., 2016) produced a regional simulation for the European domain using the regional climate model CCLM (Rockel et al., 2008). The lateral forcing for the regional simulation is from one of the global millennium simulations of the Max Planck Institute for Meteorology using their Earth System Model MPI-ESM in its COSMOS-setup (MPI-ESM-COSMOS, Jungclaus et al., 2010). The millennium ensemble includes simulations with small and large solar forcing variability amplitudes (Jungclaus et al., 2010; Fernández-Donado et al., 2013). The CCLM-simulation by Wagner used one of the large amplitude simulations. Specifically, it used the first simulation of the large amplitude ensemble (mil0021, Jungclaus and Esch, 2009; compare Jungclaus et al., 2010). The regional simulation covers the period 1645 to 1999 CE and, thus, the following discussions only deal with this period. I will refer to the regional simulation output simply by the abbreviation CCLM.

2.3 Comments on the Methods and Ensemble-approach

The PAGES 2k-PMIP3 group (2015) presents a comprehensive comparison of the recent PMIP3 ensemble of global climate simulations of the last millennium with the PAGES 2k set of continental temperature reconstructions (PAGES 2k Consortium, 2013). There was, to my knowledge, not any comparable application to a regional climate simulation. Therefore, the present document follows the collection of analyses of PAGES 2k-PMIP3 group (2015) and applies them to the comparison of a regional climate simulation and a reconstruction. I exclude those methods of the PAGES 2k-PMIP3 group (2015) focussed on detecting forcing influences and extend their setup by additional analyses on time-series properties. I use the BHM Euro 2k reconstruction of Luterbacher et al. (2016). Thus, the presented analyses are in principle another supplement to their analyses. I collect these analyses without discussion of the methods. When methods are uncommon, I give references.

Comparing the full BHM-reconstruction-ensemble with simulation data allows to highlight differences and agreement between our two main efforts of illustrating and understanding past climate changes, namely, simulations and reconstructions. However, it differs from common approaches. The ensemble allows getting a range for the analyses to assess the congruence between simulation and reconstruction. Including comparisons of time-series properties allows to assess the agreement between both data sets without considering the uncertain past forcing history of the climate system.

The presented analyses generally use regional separations comparable to those of Gómez-Navarro et al. (2015). Regional area mean series are for Scandinavia (Sca), Britain and Ireland (Bri), Central Europe (Ceu), Eastern Europe (Eeu), Iberian Peninsula (Ibe), Alps (Alp), Balkan Peninsula (Bal), Carpathian region (Car), and Turkey (Tur). Analyses additionally use the full domain series for Europe (Eur). I do not account for the different grid-resolutions, 0.5 by 0.5 degree for the simulation and 5 by 5 degrees for the reconstruction. Table 1 gives the geographical extend of the regions. Furthermore, I have to again note, that one has to be cautious in interpreting the reconstruction in regions where only sparse or no proxy input is available, e.g., south-eastern Europe. This may affect regions like, e.g., Turkey, the Balkan Peninsula, and the Carpathian region.

Table 1: Longitudinal and latitudinal dimensions of the considered regional domains. Abbreviations are for Scandinavia (Sca), Britain and Ireland (Bri), Central Europe (Ceu), Eastern Europe (Eeu), Iberian Peninsula (Ibe), Alps (Alp), Balkan Peninsula (Bal), Carpathian region (Car), and Turkey (Tur). Analyses additionally use the full domain series for Europe (Eur).

Region	Reconstruction Longitude	Reconstruction Latitude	Model Longitude	Model Latitude
Sca	7.5 to 27.5E	57.5 to 62.5N	5 to 30E	55 to 65N
Bri	-7.5 to -2.5E	52.5 to 57.5N	-10 to 0E	50 to 60N
Ceu	7.5 to 12.5E	52.5 to 52.5N	5 to 15E	50 to 55N
Eeu	17.5 to 32.5E	52.5 to 52.5N	15 to 35E	50 to 55N
Ibe	-7.5 to 2.5E	37.5 to 42.5N	-10 to 5E	35 to 45N
Alp	7.5 to 12.5E	47.5 to 47.5N	5 to 15E	45 to 50N
Bal	17.5 to 22.5E	37.5 to 42.5N	15 to 25E	35 to 45N
Car	17.5 to 32.5E	47.5 to 47.5N	15 to 35E	45 to 50N
Tur	27.5 to 32.5E	37.5 to 37.5N	25 to 35E	35 to 40N
Eur	-7.5 to 32.5E	37.5 to 62.5N	-10 to 35E	35 to 65N

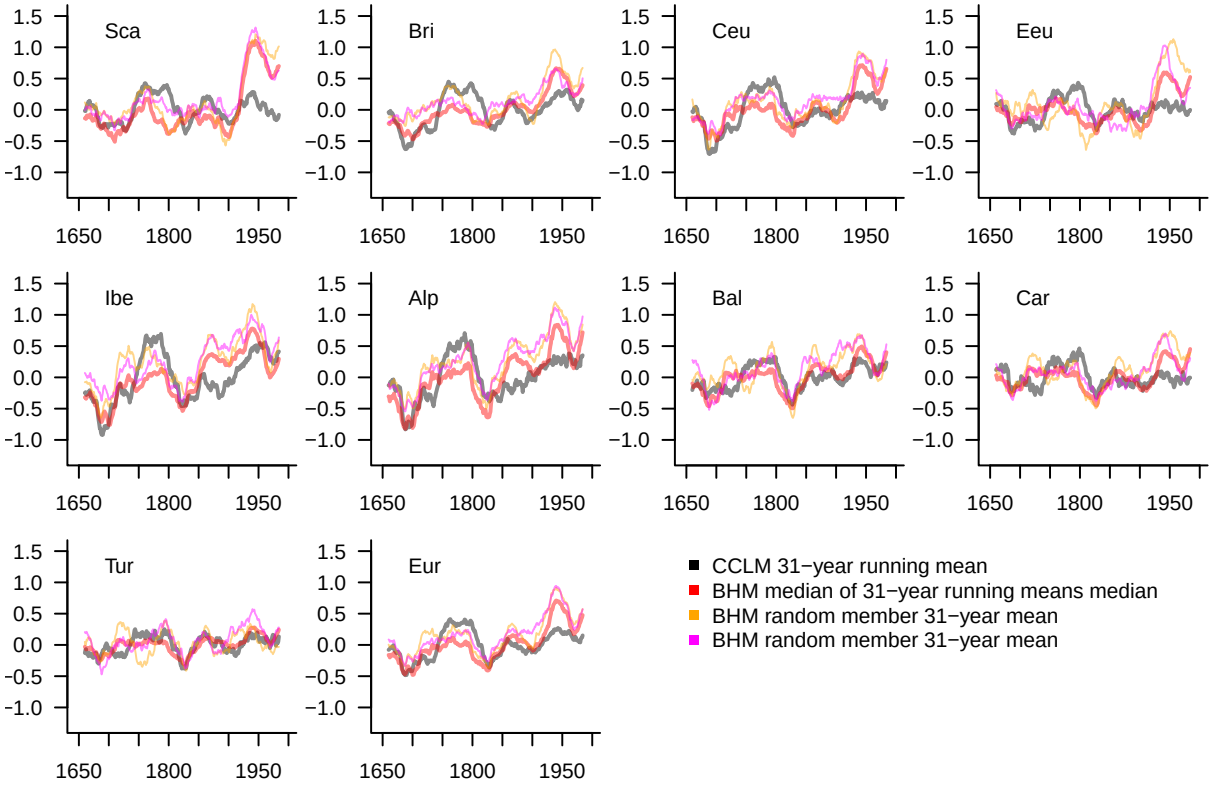

Figure 1: Temperature anomalies for regional means relative to the climatology for the period 1645-1850. Lines are 31-year running-means. Black: regional CCLM-simulation data. Red: Median of the smoothed BHM-reconstruction ensemble members. Sca: Scandinavia, Bri: Britain and Ireland, Ceu: Central Europe, Eeu: Eastern Europe, Ibe: Iberian Peninsula, Alp: Alps, Bal: Balkan Peninsula, Car: Carpathian region, Tur: Turkey, Eur: full European region. x-axes are years of the Common Era (Years CE), y-axes are temperature anomalies in Kelvin (K).

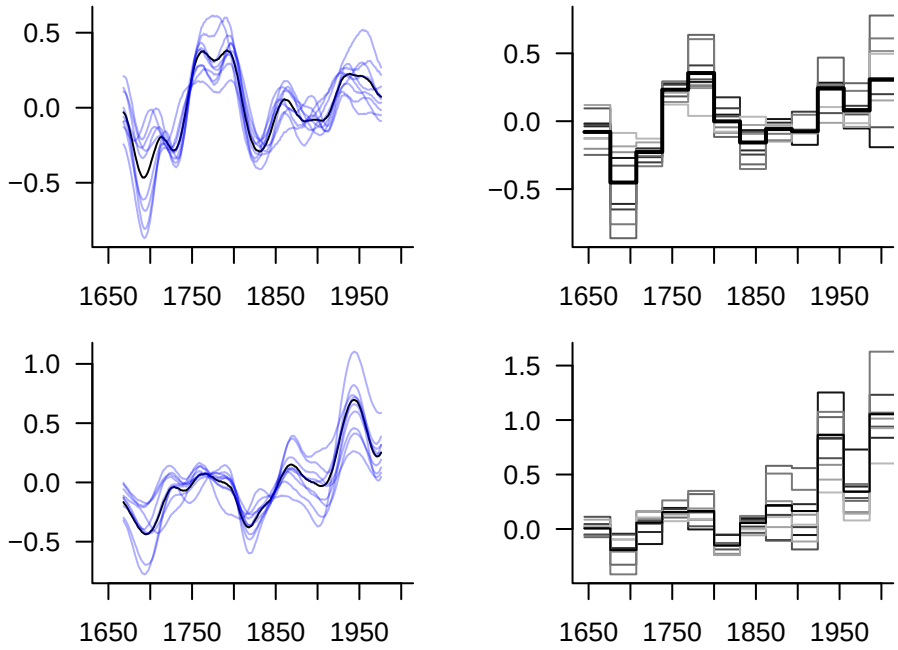

Figure 2: Comparison of smoothed regional series. Top: CCLM regional simulation output. Bottom: BHM-reconstruction. Left: 47-point Hamming-filtered data for individual regions (blue) and the full domain (black). Right: 31-year sliding mean of individual regions (grey) and the full domain (black). The BHM-median is the median of smoothed/sliding-mean series of the ensemble members. x-axes are years of the Common Era (Years CE), y-axis are temperature anomalies in Kelvin (K).

3 Comparing the Euro2k-BHM-reconstruction and the regional CCLM simulation

I generally compare the regional area average series for the simulation with the reconstruction ensemble median. The median refers to the median of the results of the analyses performed on the individual ensemble members. Occasionally I use random members of the ensemble. Since the reconstruction data is for summer means (June, July, August; JJA), all analyses consider summer data for all data sources.

3.1 Time series

Visually, 31-year running means of the time-series appear to be surprisingly similar (Fig 1). However, the visual comparison also highlights that there is no real agreement between simulated and reconstructed regional data. The plots suggest that trends are larger in the reconstruction data over the full period but multi-decadal variability may be larger in either source of information.

One striking feature in Fig 1 is the occurrence of multidecadal warmer episodes in the late 18th, late 19th and mid 20th century in simulations and reconstructions. These are more prominent in the simulation. The good congruence between the reconstructed series and the simulation data appears to be larger in the earlier part of the data. This may be due to the different trend sizes in later parts of the data and the choice of reference period. Random members of the BHM ensemble and their respective median do mostly not evolve overly diverse.

There is relatively large coherence between the different regional series within the two data sources

(Fig 2, left column) although amplitudes of variations differ notably. The non-overlapping 31-year sliding means (Fig 2, right column) emphasize the apparently larger trend in the reconstructions for some regions. The 47-point Hamming filtered series in Fig 2 appear to show less commonality between the reconstruction medians and the simulation data than the running mean series in Fig 1. I choose the 47-point window because of its comparable frequency cutoff in comparison to a 31-year moving average.

Luterbacher et al. (2016) already noted different trend sizes between some global simulations and the reconstruction and differences in the amplitude of recent warming trends. The lateral forcing of the CCLM-simulation comes from a simulation with comparatively large solar forcing amplitude from the original MPI-ESM-COSMOS millennium-simulation ensemble by Jungclaus et al. (2010). These simulations show large multi-decadal variability in recent centuries, which in part masks the long term trend.

Fig 3 shows running standard deviations over 51-year moving windows. This emphasizes the variations in standard deviations. Running measures of variability are generally very different between the data sources although some regions like, e.g., the full domain data show some similarities in the evolution of moving standard deviations.

The reconstructions indicate that variability was relatively stronger around the early 19th century. This is also seen in some simulated regional series, though generally weaker. Moving standard deviations generally differ strongly among regions.

Thus, summarising the visual agreement, the simulation and the reconstruction both show commonly a number of warmer periods during the last 400 years. Some regional data suggest common variations in the strength of their variability. Generally, neither the time-series nor their variability and trends are overly similar between reconstructions and simulations. I discuss the trends in more detail below.

3.2 Correlation analyses

In the next step, I consider correlation analyses to assess the interrelation between the ensemble members, between the ensemble and the simulation, between regions in the simulation and the reconstruction, and the evolution of interregional relations in both data sources.

3.2.1 Ensemble correlations for the period 1645-1850

Fig 4 shows intra-reconstruction-ensemble correlation histograms in red and histograms for correlations between simulation and ensemble members for the pre-1850 period. For most regions there are moderate correlations among the reconstruction members with correlation distribution modes larger than at least 0.4. The regional data for Turkey is an exception. Intra-ensemble correlations are particularly large for the Alps data.

Simulation-reconstruction correlations are generally weak but histograms show always a tendency towards positive correlations. For some regions like, e.g., the Alps or the full domain, correlations are always positive and their distribution mode is larger than 0.2. This may indicate some kind of common signal between both data sets over the period before strong anthropogenically forced trends.

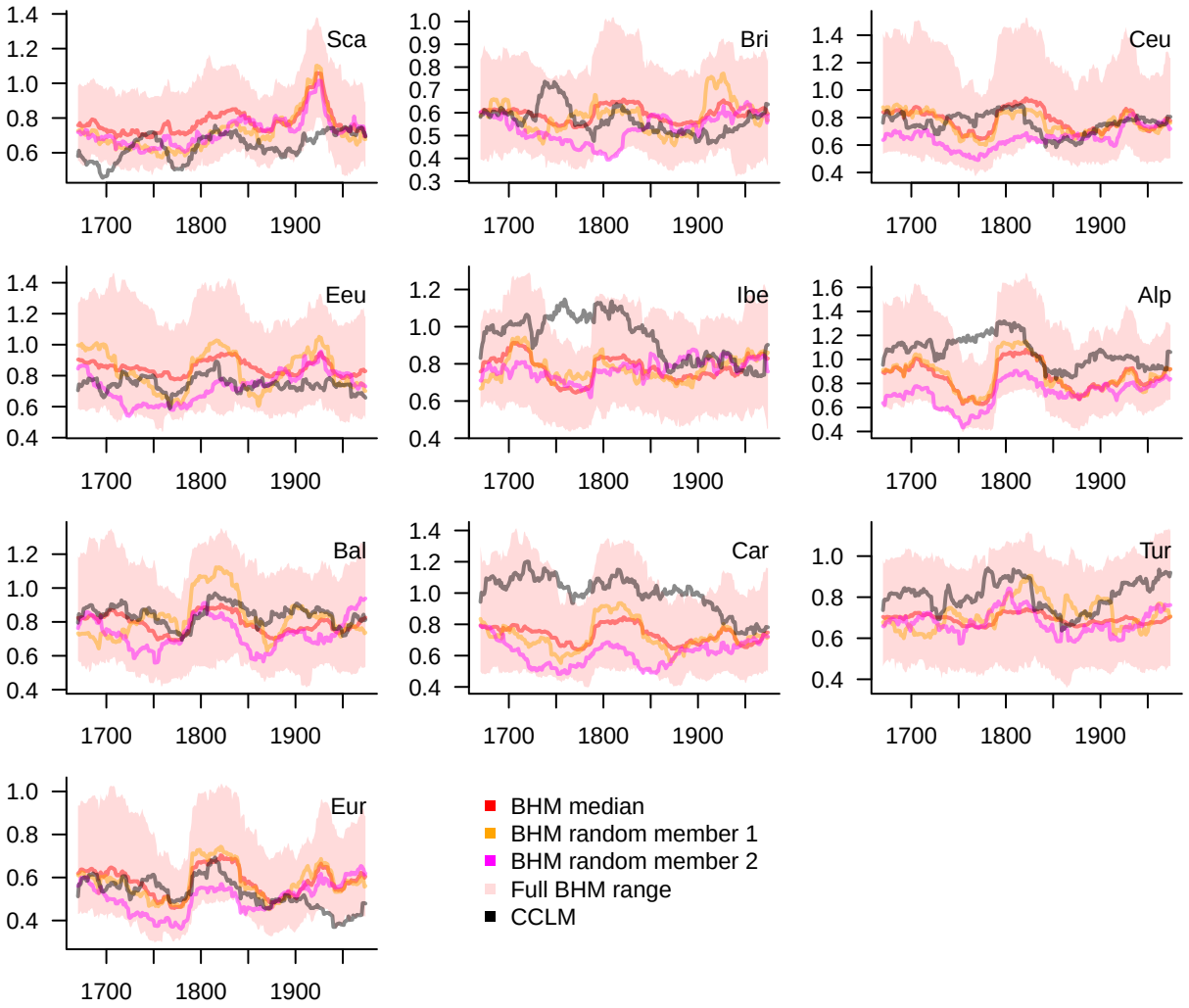

Figure 3: Comparison of 51-year running standard deviations for the CCLM regional simulation, the median of the smoothed BHM-reconstruction ensemble-analyses and two random members of the ensemble. x-axes are Years CE, y-axes are Standard Deviations in degree Kelvin.

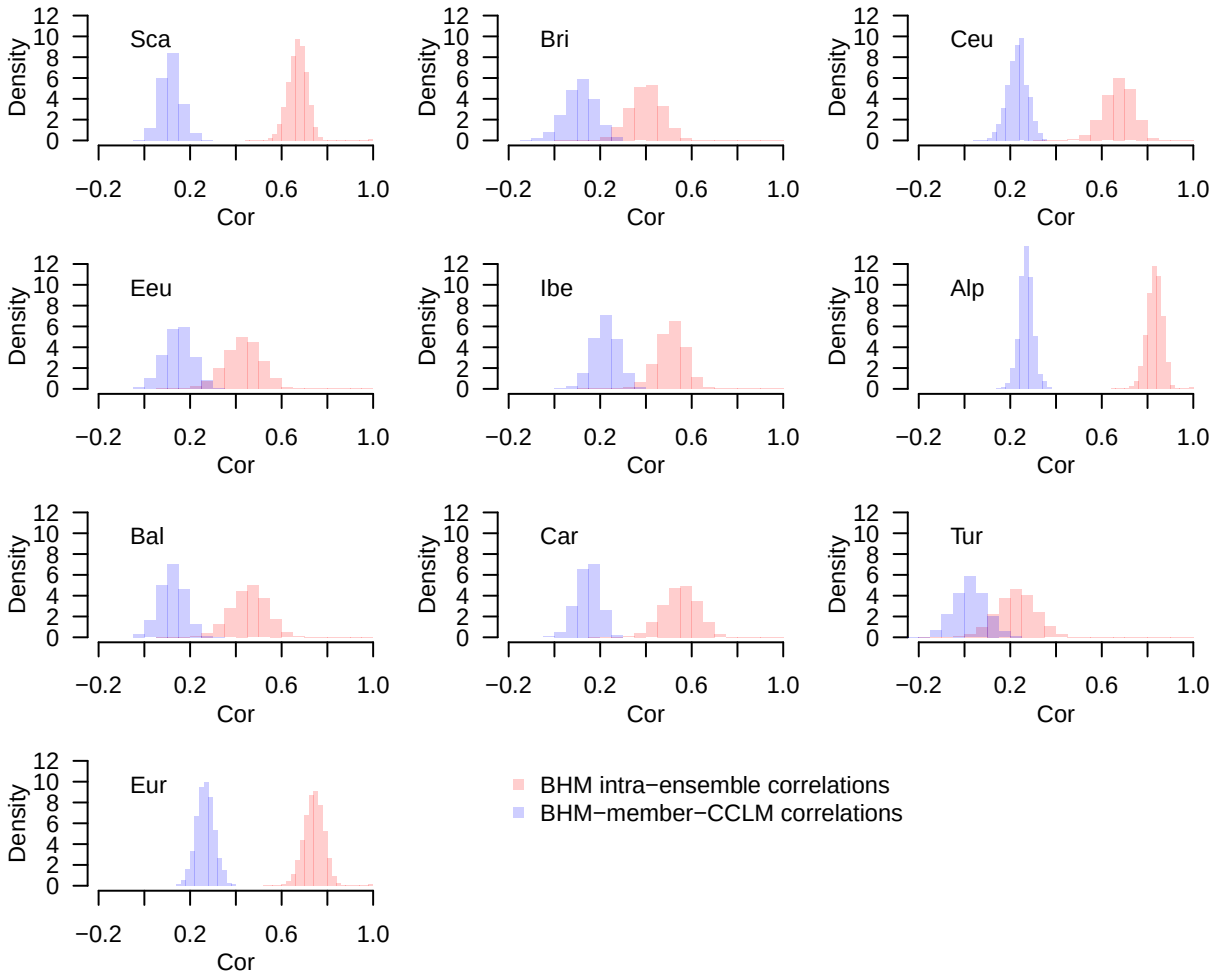

Figure 4: Correlation coefficients between BHM-reconstruction ensemble-members (red), correlations between BHM-reconstruction ensemble-members and the simulation (blue). Correlations are over the pre-1850 period only.

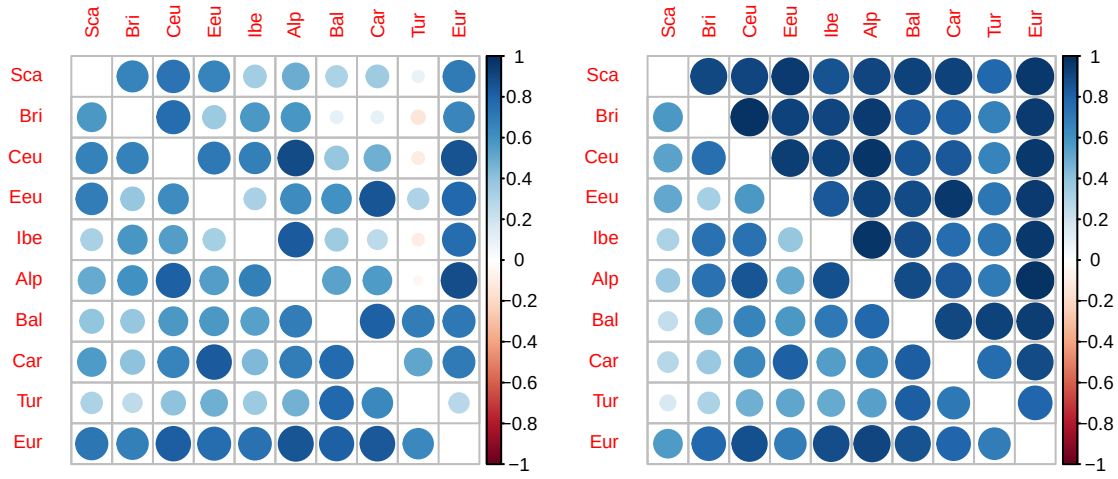

Figure 5: Interregional correlations for, left, the unsmoothed data, right, 31-year running mean series. Upper triangles of matrices are for the regional CCLM simulation, lower triangles are the median of the BHM-reconstruction analyses. Correlations are over the pre-1850 period only.

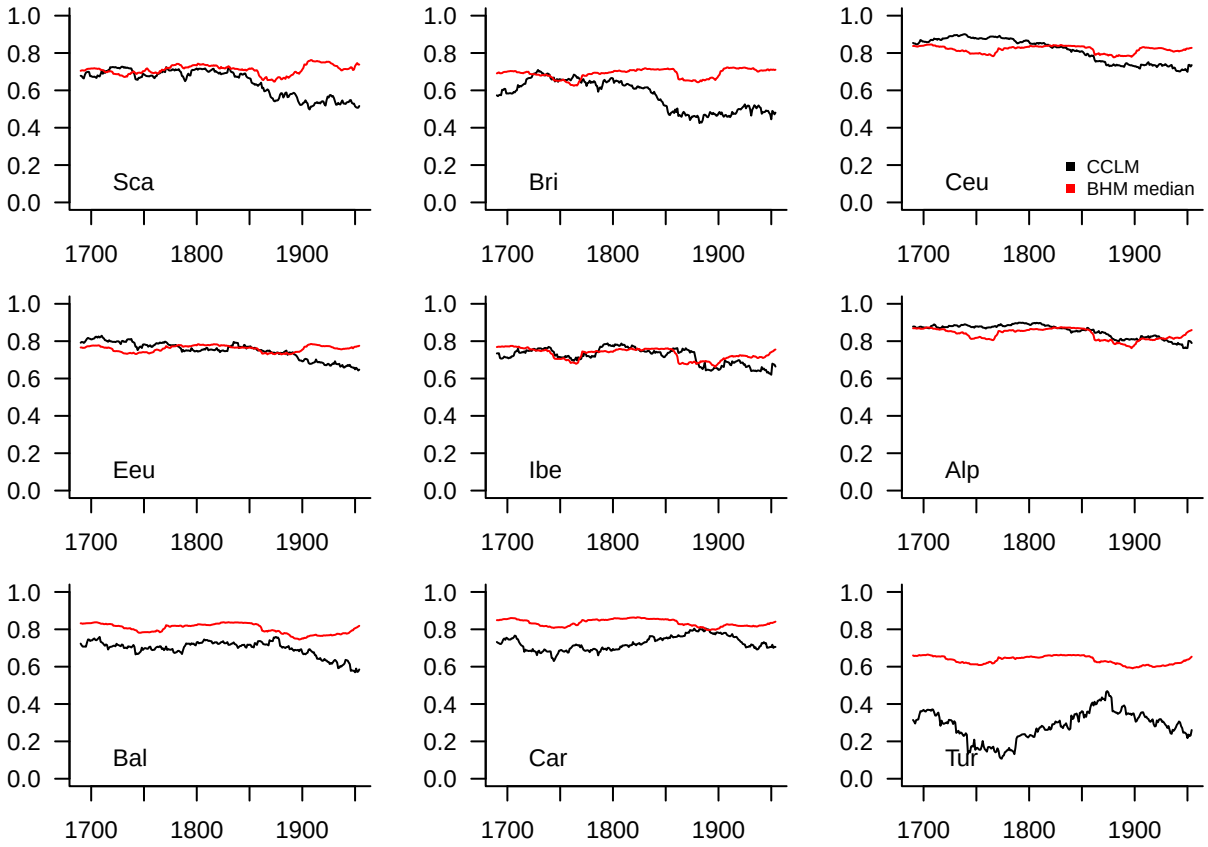

Figure 6: Running correlations between regional series and the full domain series over 91-year moving windows. Black, regional CCLM-simulation, red, median of analyses for the BHM-reconstruction ensemble.

3.2.2 Interregional correlations

Fig 5 shows the interregional correlations as correlation-matrix plots. Lower triangles are for the median of reconstruction ensemble member correlations, and upper triangles are for the simulation.

Correlations are diverse among regions for the unsmoothed data for both sources of information (Fig 5, left panel). Correlations become more homogeneous for the simulation data if they are smoothed but remain quite diverse for the median of analyses on the smoothed reconstruction ensemble.

Correlations are generally weakest for the Turkey region for both datasets in the interannual data and the smoothed data (Fig 5). This behaviour is least pronounced in the smoothed simulation data. Turkey also correlates least with the full domain series.

Interregional correlations generally increase for the simulations with larger amount of smoothing (Supplementary Fig 22 in the Appendix). Only minor dips occur for very long smoothing windows and correlations with the Turkish series.

Contrarily, results for the reconstruction series show a varied behavior in their median with notably weak correlations throughout regions and window lengths (Supplementary Fig 23 in the Appendix). Noteworthy is particularly the Scandinavian data, which shows an up-and-down variation with increasing smoothing.

3.2.3 Running correlations

Running correlations allow to clarify how interrelations change over time. Correlating the unsmoothed series over short windows gives a rather noisy picture (not shown). Fig 6 shows the running correlations between the unsmoothed regional series and the full domain series over 91-year windows. Most reconstructed series have weaker correlations with the full domain over a period centred around the early to mid-18th century. A second weakening of correlations occurs in most series in the late 19th century. Simulated series mostly show a notable weakening after about 1850. Some simulated records also have weaker correlations in the mid-18th century. Correlations are occasionally weaker for the simulated data compared to the reconstructed series not only in the late part of the data.

If I consider correlations between 47-point Hamming-filtered series (not shown), the simulated series show some similarities with the reconstructed series though excursions are occasionally shifted in time. Particularly, there are then periods with comparably weaker correlations in simulation and reconstruction. One hardly can identify this synchrony in Fig 6 except possibly for the Iberian peninsula. However, moving correlations of smoothed series artificially accentuate features.

In summarising the correlation results, intra-ensemble correlations are notable, but correlations with the simulation data are always weak though generally positive. Inter-regional correlations are usually stronger in the simulation data, which fits the common finding of larger inter-relations in simulated data compared to reconstructions (compare, e.g., PAGES 2k-PMIP3 group, 2015). Moving correlations with the full domain also differ between simulation and reconstruction. Interestingly, there are periods of weak correlations particularly for the simulation. The changes in correlation may relate to the observed changes in variability in the regional series (compare Fig 3).

3.3 Trends

Figs 7 and 8 summarise moving window linear trends of different lengths for the simulation and the reconstruction ensemble, respectively. As I do not show observations for comparison, the panels only highlight the differences between simulated and reconstructed trends. Note, observational regional data is not available in acceptable quality over the full period. Luterbacher et al. (2016) have already shown the relative good agreement between instrumental data and reconstructions for the domain mean data, though not for the trends.

While the trends for the reconstructed data are stronger in recent windows, overall there are not any overly obvious contrasts between simulation and ensemble trend medians. The Figs show the different size of trends in both data sources but also highlight that both show similar patterns of trends. These similarities possibly reflect our understanding of the past climate forcing history by solar, volcanic, and anthropogenic drivers (compare, e.g., Jungclaus et al., 2010; Fernández-Donado et al., 2013; Schmidt et al., 2011).

Supplementary Figs 24 and 25 plot the moving window 201 and 151-year trends respectively in the Appendix. They show the regional CCLM-simulation data, the median of the calculated trends for the reconstruction data, two random members of the reconstruction ensemble, and the full reconstruction ensemble range. 201-year trends often show differences between the simulation and reconstruction data, but occasionally also agree quite well for some regions. Reconstructed trends are generally larger than the simulated ones in the later part of the data. Already the smoothed time-series in Fig 1 indicate this. Differences are often slightly less prominent over 151-year windows but occasionally there still are strong deviations particularly in the central part of the data.

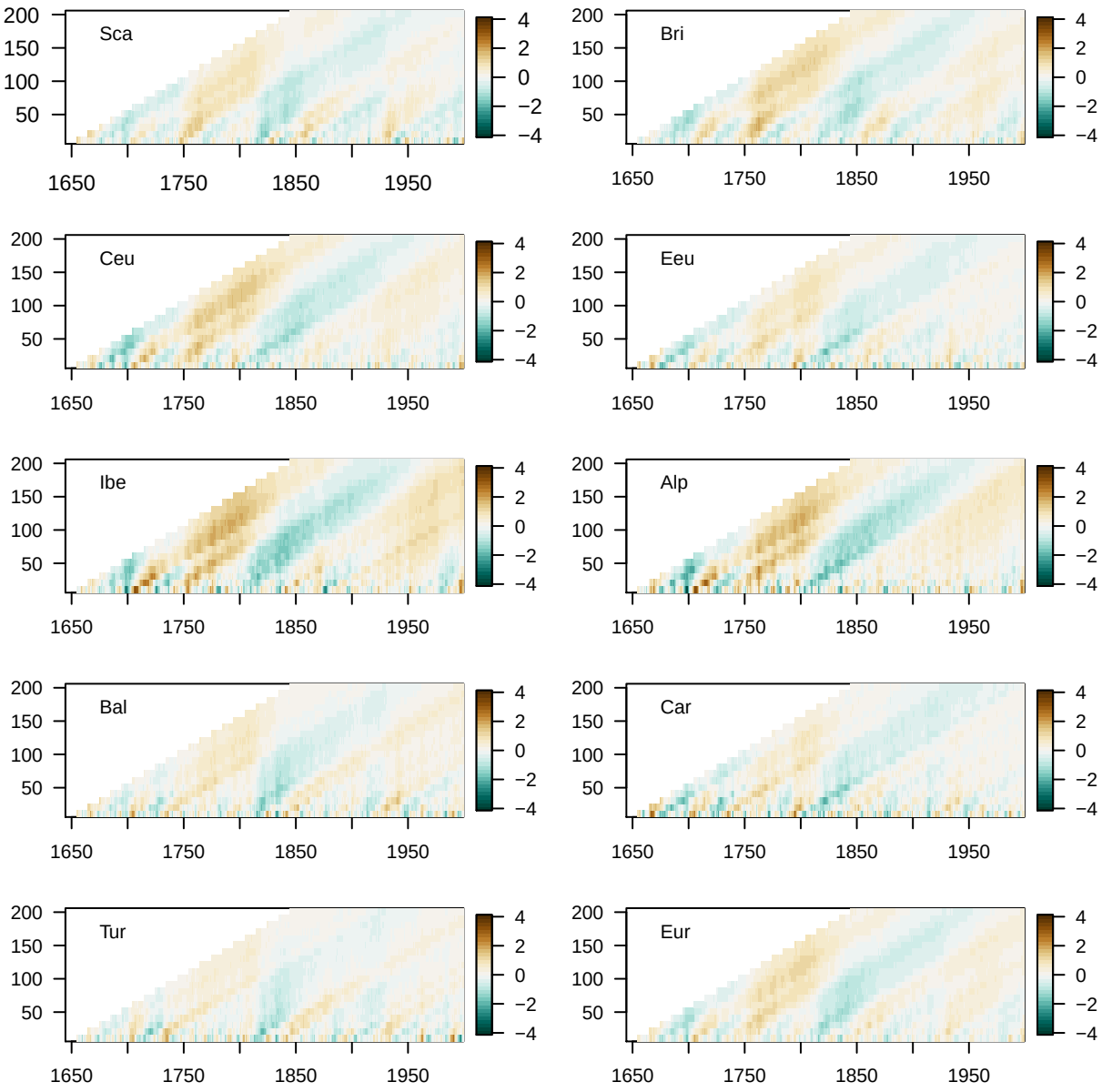

Figure 7: Comparison of moving linear trends of different window lengths for the regional CCLM simulation. Shading is for Kelvin per window-length. Window-lengths are 11 to 201 years in 10 year steps.

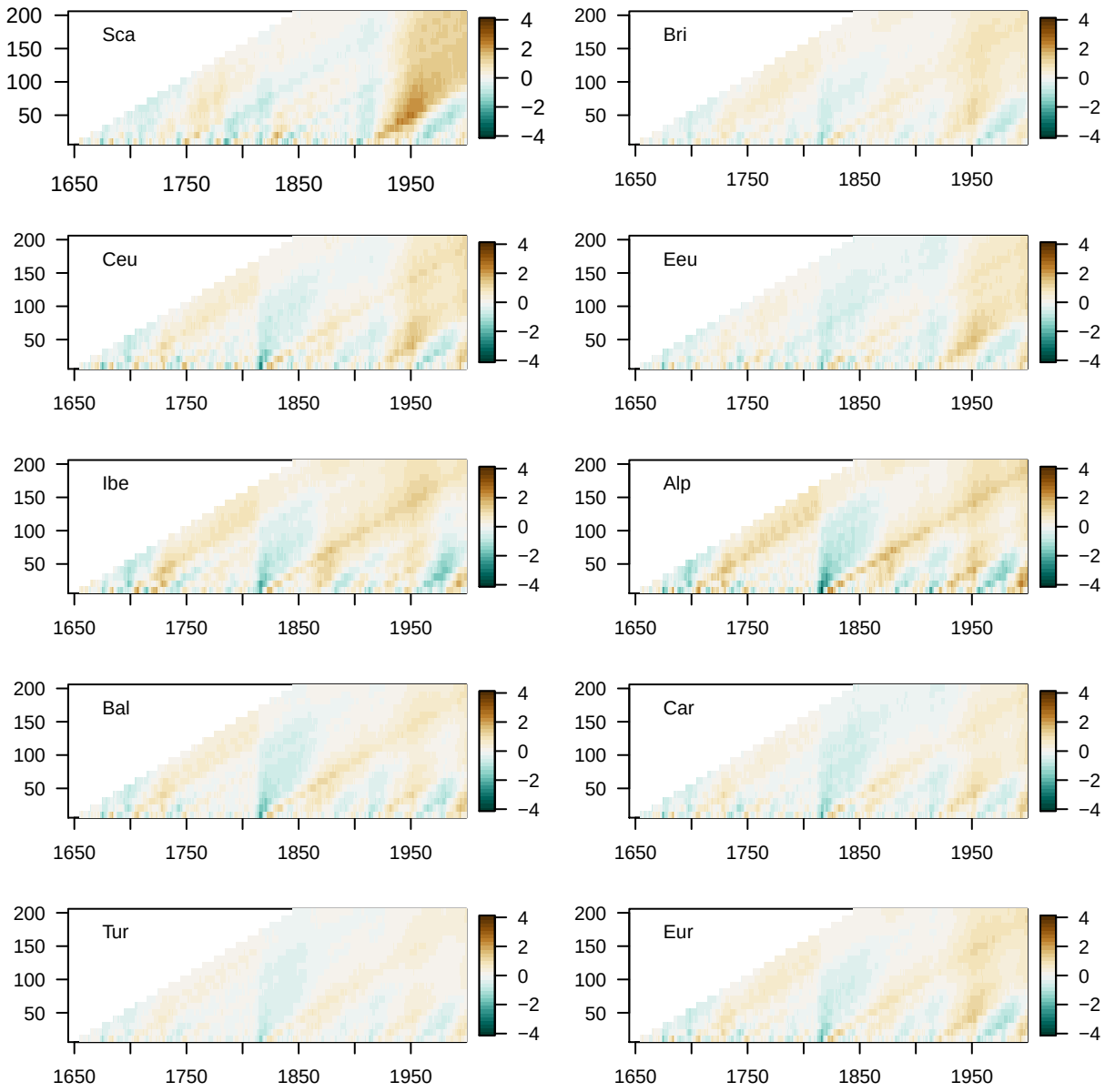

Figure 8: Comparison of moving linear trends of different window lengths for the reconstruction ensemble. Shown is the median of analyses for individual members. Shading is for Kelvin per window-length. Window-lengths are 11 to 201 years in 10 year steps.

Thus, trends in both data sources generally reflect our knowledge of past climate forcing and boundary conditions in the region of interest, i.e. Europe. Disagreement in timing and trend sizes, especially over long trend periods, may be, among other things, due to internal variability, the uncertainty in forcing data, the specific implementation of the forcing in the model, and the inability of a low top model to reproduce dynamical top-down processes originating in the middle and upper atmosphere (compare, e.g., Jungclaus et al., 2010).

3.4 Consistency

Annan and Hargreaves (2010) highlight the usefulness of the concept of ensemble reliability or ensemble consistency for climate studies. It was previously mainly used in forecast verification. For applications see also, e.g., Hargreaves et al. (2013). Jolliffe and Primo (2008), Anderson (1996), and Hamill (2001) provide relevant discussions of probabilistic consistency and rank histograms, while Marzban et al. (2010) introduce the concept of climatological forecast consistency and residual quantile-quantile plots. Previous simulation-reconstruction comparisons include, e.g., the PAGES 2k-PMIP3 group's work (2015).

Consistency assessments rely on the paradigm of a statistically indistinguishable ensemble (e.g., Annan and Hargreaves, 2010). For this, one assumes a validation target and an ensemble of data to be exchangeable samples from a common distribution.

Climatological consistency describes the similarity of the climatological probability distributions of the target and the ensemble over a selected period. Plotting the residual quantiles between the target and the ensemble helps to visualize this. To be more specific, classical quantile-quantile plots display the quantiles of one distribution against the quantiles of another, potentially theoretical distribution. Residual quantile-quantile plots display the differences between the pairs of both quantile series against the target quantiles. Thus, values of or close to zero for all residual quantiles signal consistency.

Probabilistic consistency analyses identify the position of the target within the range of the ensemble. Rank histograms traditionally are an appropriate visualisation for such analyses. In this case, one orders the values of the ensemble and the target for a data point, identfies the position, i.e. the rank, of the target, and then plots counts of these ranks over all data points in histograms. A flat rank histogram signals probabilistic consistency.

3.4.1 Climatological consistency

Fig 9 displays the climatological consistency assessment for the ensemble reconstruction relative to the simulation data for the pre-1850 period. I plot the frequencies of residual quantiles between the reconstruction ensemble and the 'target' simulation data. An alternative approach would plot a series of residual quantiles for each ensemble member.

Unsurprisingly the extreme quantiles spread widely. Concentrating on the more confined central quantile residuals, there are mainly three behaviours of the data. For one, regions like Britain and Ireland, Central Europe, Eastern Europe, and also the full domain data show consistent residuals, i.e. they are close to zero. However, the Iberian Peninsula, the Alps, the Carpathians, and less strongly the Balkan and Turkey show an underdispersive behavior, residuals have a negative trend. That is, the distributions of the reconstruction are usually narrower than the simulation data, their variance is smaller.

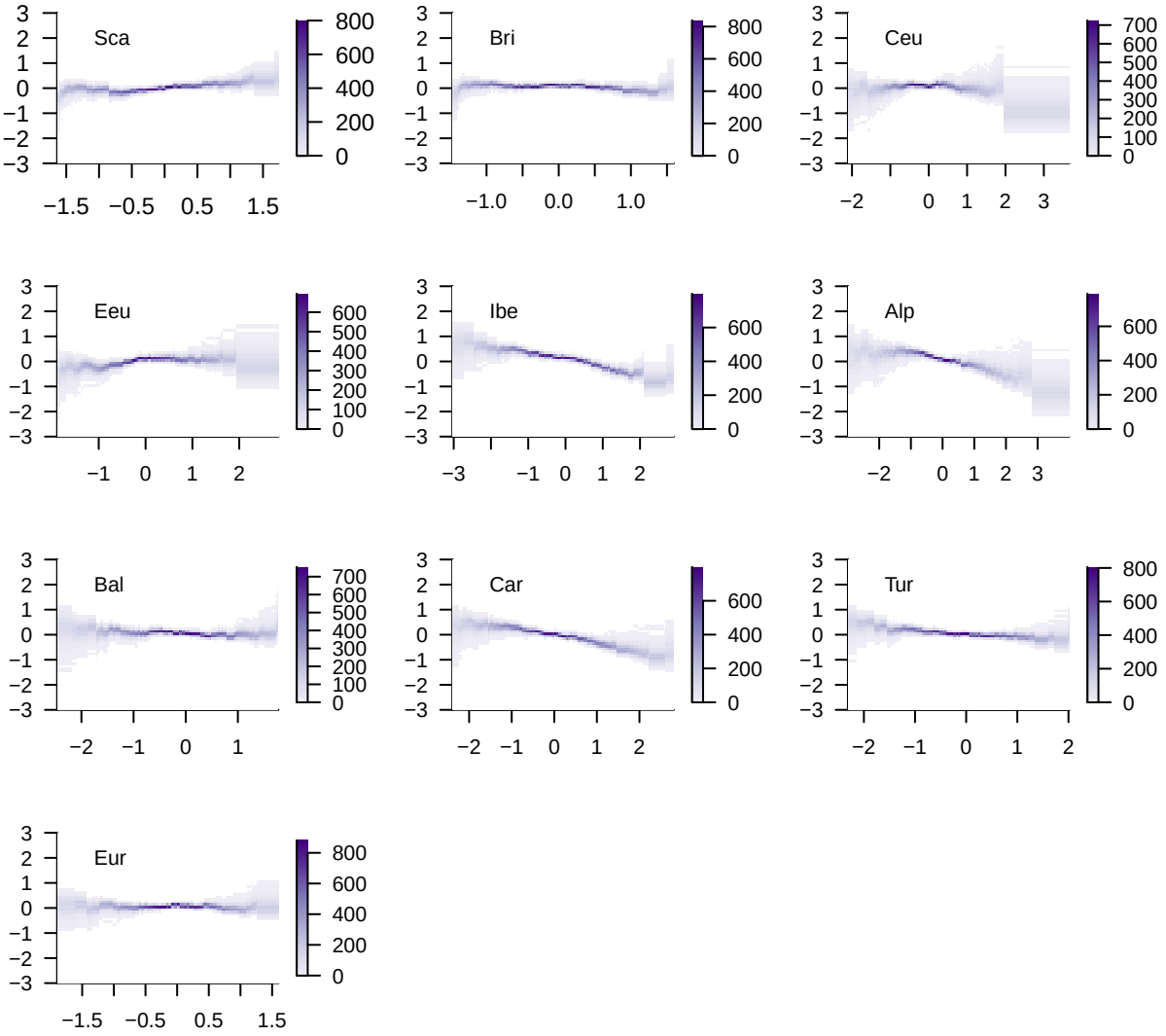

Figure 9: Climatological consistency of the BHM-reconstruction ensemble relative to the regional CCLM simulation as seen in residual quantile-quantile plots (Marzban et al., 2010). Residual quantile-quantile plots differ from classical quantile-quantile plots by plotting the difference between the quantiles of interest and the target quantiles against the target quantiles instead of plotting the quantiles of interest against the target quantiles. x-axes are anomaly quantile values in Kelvin, y-axes are residual quantiles in Kelvin. Shading are count frequencies.

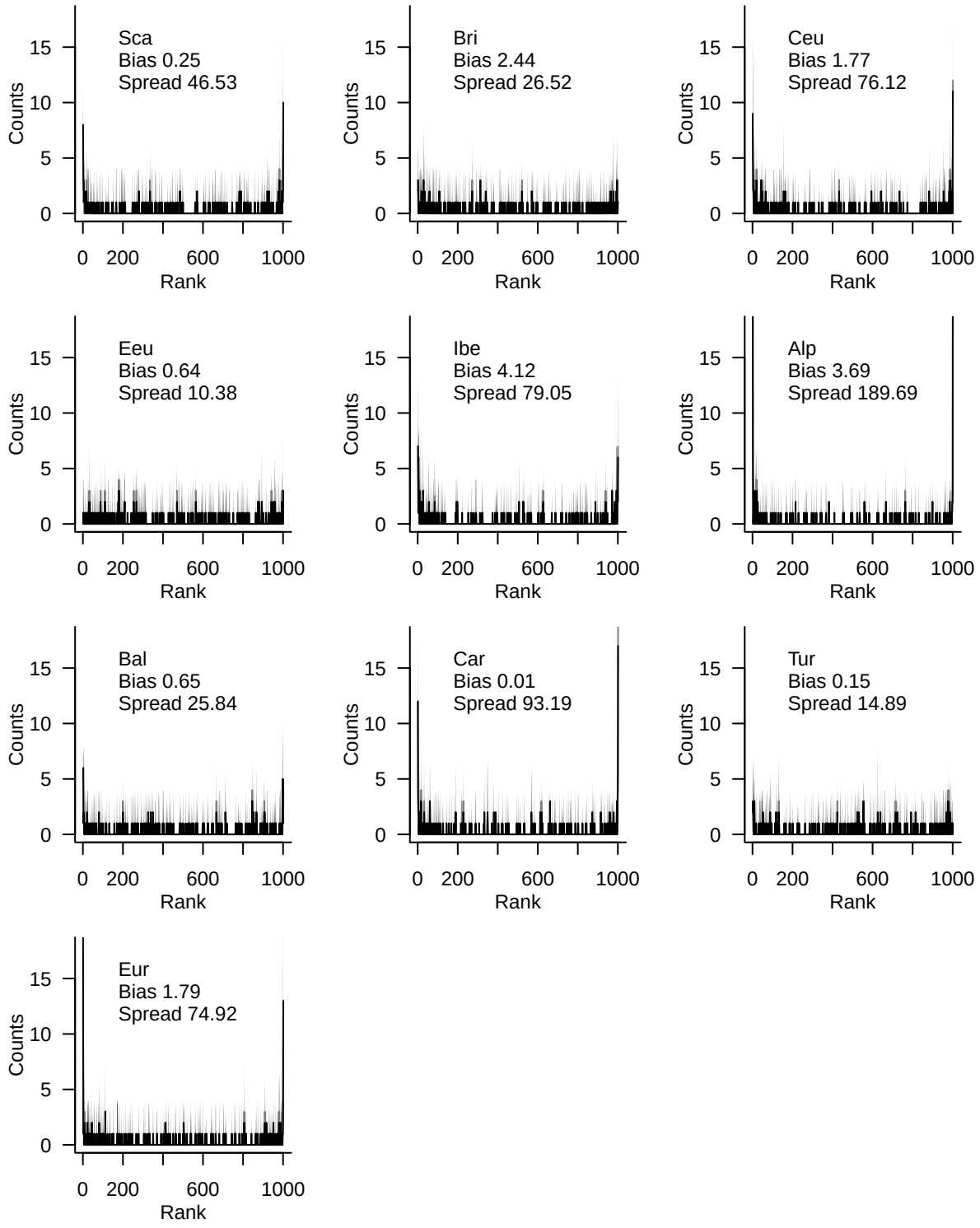

Figure 10: Probabilistic consistency of the BHM-reconstruction ensemble relative to the regional CCLM simulation. The panels show for each region rank histograms, i.e., the rank counts of the simulation target relative to the ensemble. Numbers are bias and spread measures following Jolliffe and Primo (2008). For details of the method compare, e.g., Annan and Hargreaves (2010), Hargreaves et al. (2013), Jolliffe and Primo (2008), Anderson (1996), Hamill (2001), Marzban et al. (2010), or the PAGES 2k-PMIP3 group's work (2015).

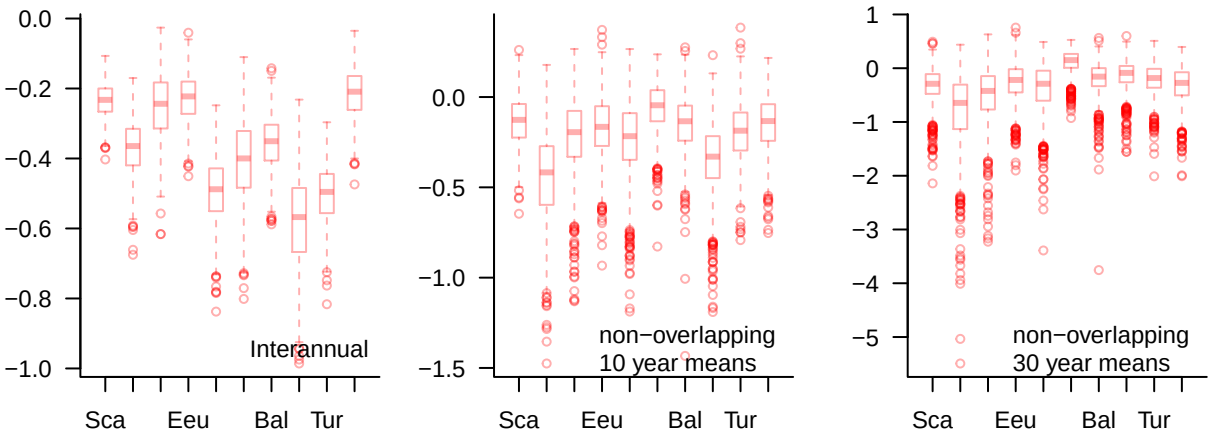

Figure 11: Skill of the BHM-reconstruction ensemble members to capture the regional CCLM simulation variability compared to a no-change reference. y-axes are nondimensional skill-measures. Left panel: boxplots for interannual data; central panel, boxplots for non-overlapping 10 year means; right panel, boxplots for non-overlapping 30 year means.

This behaviour is strongest for the Iberian Peninsula. Thirdly, Scandinavia shows a slight tendency to the opposite. Such a positive trend signals overdispersion. That is, the variance of the reconstruction data is larger than for the simulation. Nevertheless, it seems appropriate to say that there is not general (climatological) inconsistency between the data. However, the data are anomalies and thus do not include potential biases.

3.4.2 Probabilistic consistency

Keeping in mind, that Marzban et al. (2010) highlight how intra-ensemble and ensemble-target-correlations can influence rank histograms, Fig 10 shows rank histograms to assess the probabilistic consistency of the reconstruction ensemble relative to the simulation. Fig 4 above shows the correlations for the BHM-ensemble and between ensemble and simulation.

Most regions give strongly overdispersive rank histograms, i.e. the 'target' falls too often outside the ensemble range. While some histograms may visually suggest a flat behavior, the size of measures for spread-deviations allows to reject probabilistic consistency for all regions (compare Jolliffe and Primo, 2008).

Note, that I use very sparse histograms. Only about 200 measurements are available for ranking in the 1001 classes. This affects statistics and implies that small counts are enough to result in an overdispersive histogram. On the other hand, it also emphasizes the finding that the target is often outside of the ensemble range. However, the analyses of Marzban et al. (2010) suggest that rank histograms for ensembles with strong intra-ensemble correlations but relative small ensemble-target correlations are likely to be overdispersive.

In summarising, there is not general climatological inconsistency. Similarly, spread-deviations allow to reject probabilistic consistency, but the large intra-ensemble correlations also prevent to declare the rank-histograms generally inconsistent.

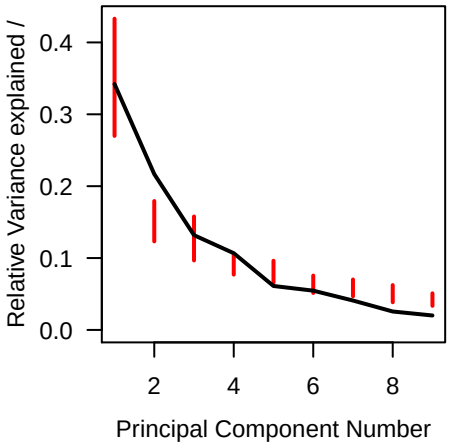

Figure 12: Variance explained by the principal components. Red, range of the BHM-reconstruction ensemble, black, regional CCLM simulation.

3.5 Skill-analysis

The PAGES 2k-PMIP3-group (2015) also adapted the concept of skill analysis for reconstruction-simulation comparisons from Hargreaves et al. (2013). Here, I use a very simple skill measure to assess how the BHM-ensemble is able to capture the target CCLM simulation compared to assumptions of no change. Negative values indicate that the ensemble of reconstruction-series has no skill in representing the simulated data compared with the no-change-reference.

The boxplots for skill measures of the ensemble members in the left panel of Fig 11 indicate that the ensemble lacks skill considering unsmoothed interannually resolved data. If I use means over non-overlapping windows of 10 or 30 years, there are some reconstruction ensemble members, which show skill. Note the different axis scales for the three panels as deviations increase at the same time with increasing window lengths. There is no pattern in the increase in skill measure, it remains unclear whether skill may be more likely or larger for certain regions.

3.6 Principal component analysis (PCA)

Analyses, so far, only considered individual data series or pairs of data. In the following, a principal component analysis (PCA) supplements them by providing more information about the interrelations among the regions. It summarises the covariability among the regional subdomains of the reconstructions and the simulations.

Note, I perform the PCA separately for simulation and reconstruction. Thereby, the comparison of time-series uses projections on different loadings. That is, the comparison of the patterns and of time-series do not complement each other. An alternative approach would be to, first, compare the loadings and, then, project the data on a common set of loadings to compare the evolution with respect to this loading. Such a comparison would more appropriately consider the evolution of a certain set of modes. However, as there is no guarantee that such a common set of modes is valid for all data sets, I compare the projections within each data set and refrain from making strong interpretations.

The first principal components for both datasets explain about 35% of the variability (Fig 12). The second PCs explain about 15% for the reconstruction but over 20% for the simulation. The ensemble range does not include the simulation for the second principal component and some higher order PCs.

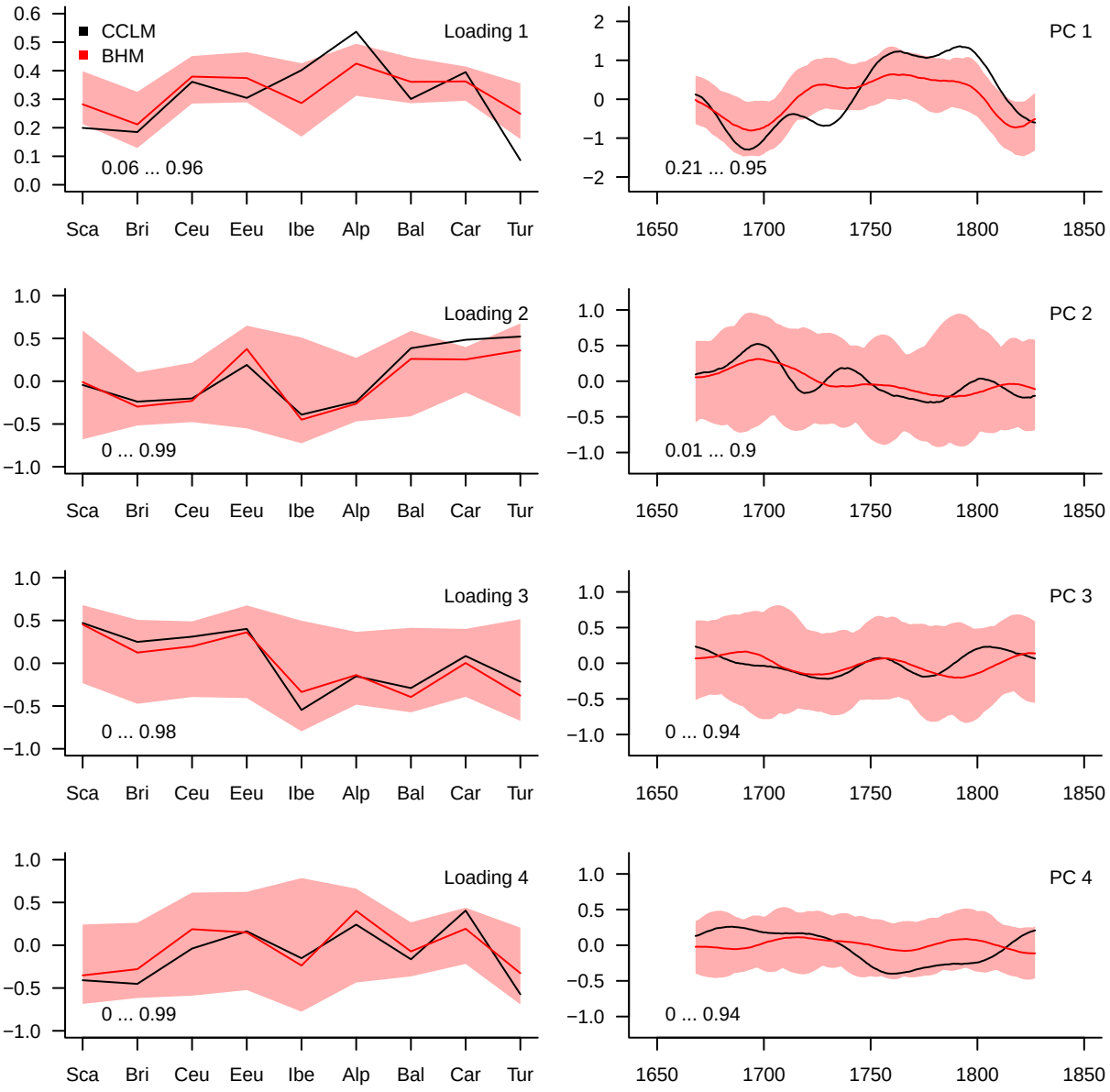

Figure 13: Principal component analysis over the regional series for principal components 1 to 4 from top to bottom. Left: Loading. Right: 47-point Hamming-filtered time series. Shading is the full range of the reconstruction loadings and the smoothed reconstruction time-series. The red line is the median. The black line is for the simulation output. Numbers in the bottom left corner are the range of correlations between the simulation-PC and the reconstruction ensemble PCs. y-axes are non-dimensional values. x-axes for the loadings are the regions, and years CE for the time-series.

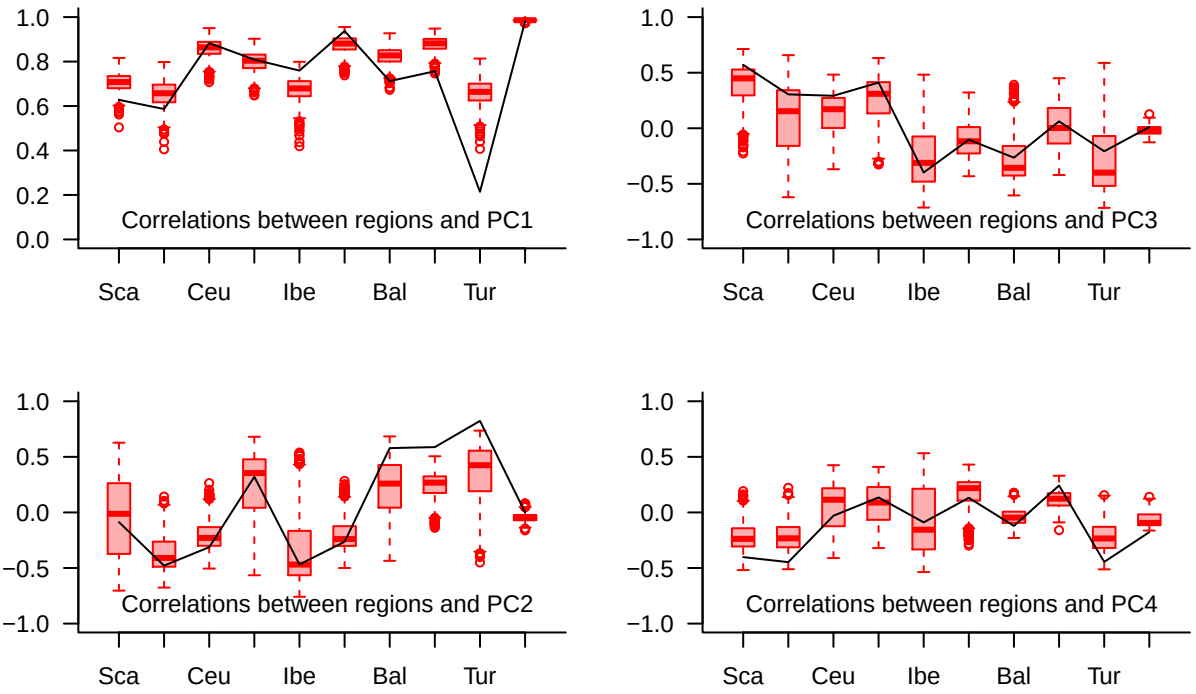

Figure 14: Correlation coefficients between the regional series and the principal component series. Boxplots are for the BHM-reconstruction ensemble. The line is for the regional CCLM simulation.

Principal component loadings are similar between the reconstruction and the simulation (Fig 13, left column) except possibly for PC1. The most notable difference is the relation between the Iberian Peninsula and Eastern Europe and the Alps in PC1. However, for principal component patterns 2 to 4 there is a large range for the reconstruction ensemble.

Interestingly, the smoothed PC time series also show some general resemblance (Fig 13, right column). However, there are also pronounced differences especially for PC1 and PC4, which is to be expected considering the smoothed time-series in Fig 2. Again, some time-series, e.g. PC2, have a wide range for the reconstruction ensemble. Nevertheless, these results suggest that leading modes of variability are comparably captured in both the simulation and the reconstruction for the pre-1850 period for the spatially coarse resolution setup of nine regional average series.

I show the unsmoothed PC time series in the Appendix (Supplementary Fig 26).This Fig highlights that amplitudes of median series are small for PCs 2 to 4 for the reconstruction, i.e., that variations and variability differ strongly between ensemble members.

Fig 14 shows the relation between the regional series and the PC time series differently by plotting the correlations between the regional series and the PC series. As for the PC loadings and the PC time series, correlations are comparable between the simulation and the reconstruction. The correlations also follow similar patterns - which is possibly to be expected as the PCs base on the covariability among regions.

For PC1, largest differences between simulation and reconstruction occur for the Turkey-region. The Turkey-series also shows the weakest correlations with PC1 and the largest spread in correlations with PC2, while PC3 correlations are largest for this data. It is worth noting that the full domain series correlates nearly perfectly with the first PC time series.

In summarising, the modes of variability appear comparable in reconstruction ensemble and simulation. However, I do these analyses on a spatially coarse setup of nine regional average series, and

perform the analyses on simulations and reconstructions independently.

3.7 Time series properties

3.7.1 Spectral densities

Fig 15 plots sample spectral density estimates for the simulation data against analyses for all ensemble members. Envelopes of the reconstruction ensemble spectral densities are generally wide over the full frequency range for all regions. Spectral density estimates for the simulation fall mostly inside these envelopes.

There are few clear differences between reconstruction and simulation spectra. Some reconstructed regional series ensembles show a maximum in the densities at frequencies approximately equivalent to a seven year period, which is missing in the simulation data.

Generally the comparison of the simulation spectral densities with the ensemble range indicates a lack of disagreement, which is in line with the visual assessment of comparable variability on high and low frequencies in simulation and reconstruction series. However, this cannot necessarily be interpreted as agreement of spectral properties of the data.

3.7.2 Hurst exponent

The Hurst coefficient (e.g., Weron, 2002) is a measure of self-similarity or long-range dependence of a time-series. Economics and hydrology use it commonly but the paleoclimatology-community also got interested in recent years (e.g., Bunde et al., 2013). Weron (2002) discusses uncertainty of the estimation process.

Fig 16 summarises estimates of the Hurst coefficients of the reconstruction and simulation data. Hurst-exponents for the simulation data are within the range of results for the reconstruction ensemble, which itself is confined to values larger than 0.5 but smaller than 0.8, i.e., there is usually some amount of long-term positive auto-correlation in the time-series.

Uncertainty of individual estimates is obviously large since the time-series are relatively short. Furthermore, the reconstruction-method may imprint certain time-series properties onto the data. Nilsen et al. (2018) discuss how the assumptions of the reconstruction method potentially result in a reconstruction more in line with the assumed time-series characteristics than with the real input time-series characteristics. The similarity in Fig 16 nevertheless suggests some agreement in self-similarity between simulations and reconstructions over the considered period.

3.7.3 Autoregressive (AR) order

Fig 17 summarises fits of autoregressive (AR) processes to the reconstructed and simulated regional time-series. The Fig further shows results for forced fits of AR-processes of order 1.

Fits suggest an order of 1 for the majority of ensemble members for all regions. However, fits to the simulation data give larger orders than for the bulk of the ensemble-members for the most regions. This points to larger autocorrelation in the simulation-data. Only Turkey and the Carpathian region give orders of zero for the simulation data and the Balkan gives an order of 1.

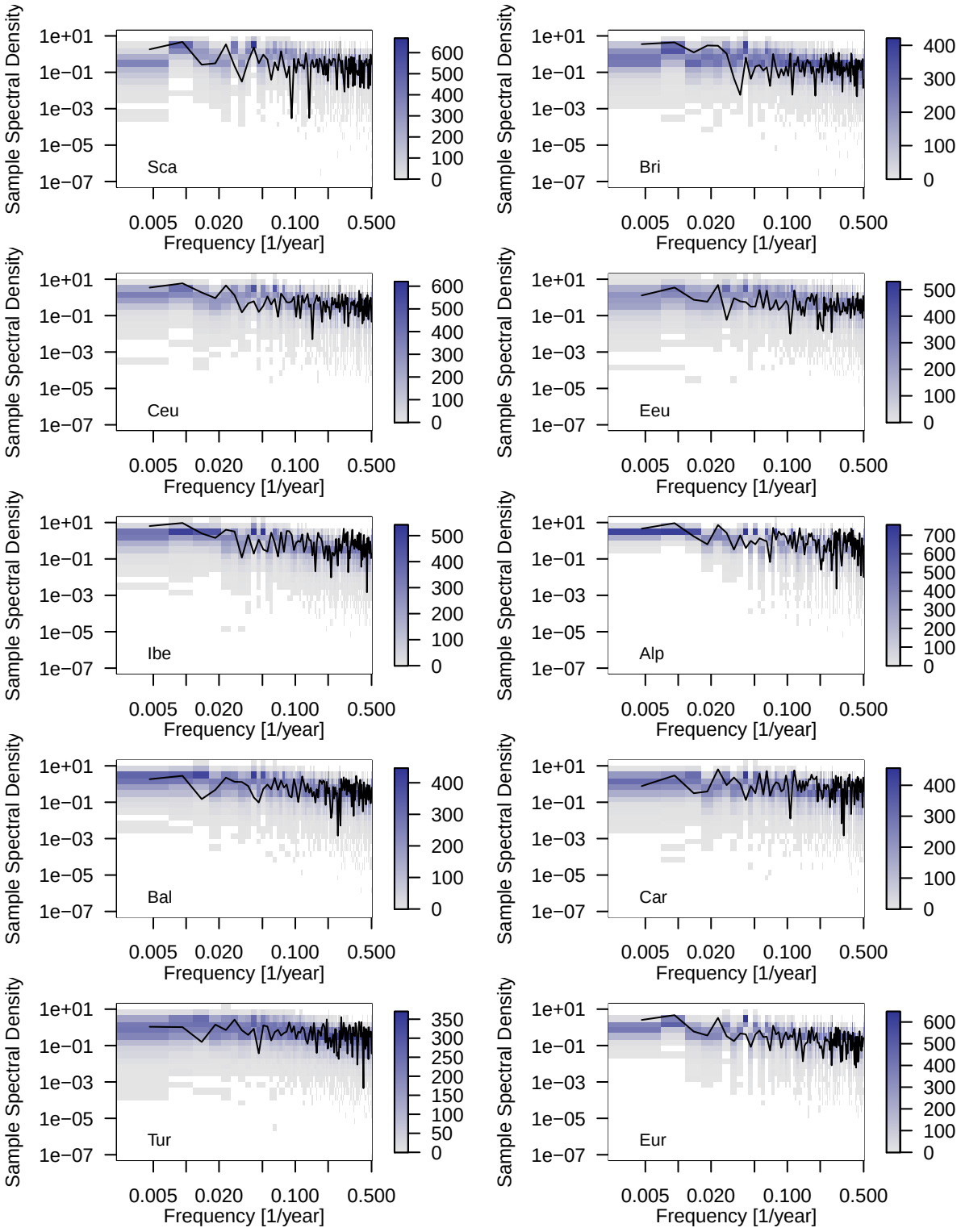

Figure 15: Comparison of the spectral density of the simulation (black line) and the frequency of spectral density estimates of the ensemble members (shading).

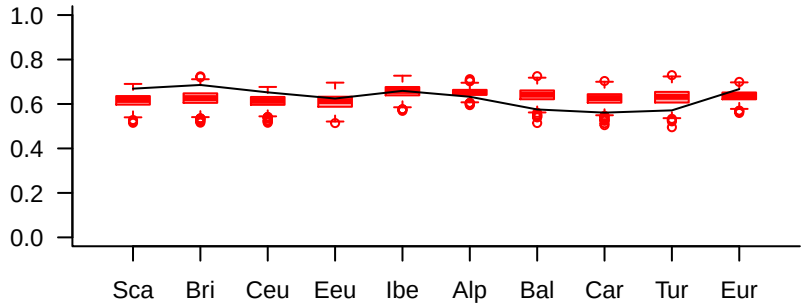

Figure 16: Boxplot of Hurst coefficients for the reconstruction ensemble. Black line is for the simulation data.

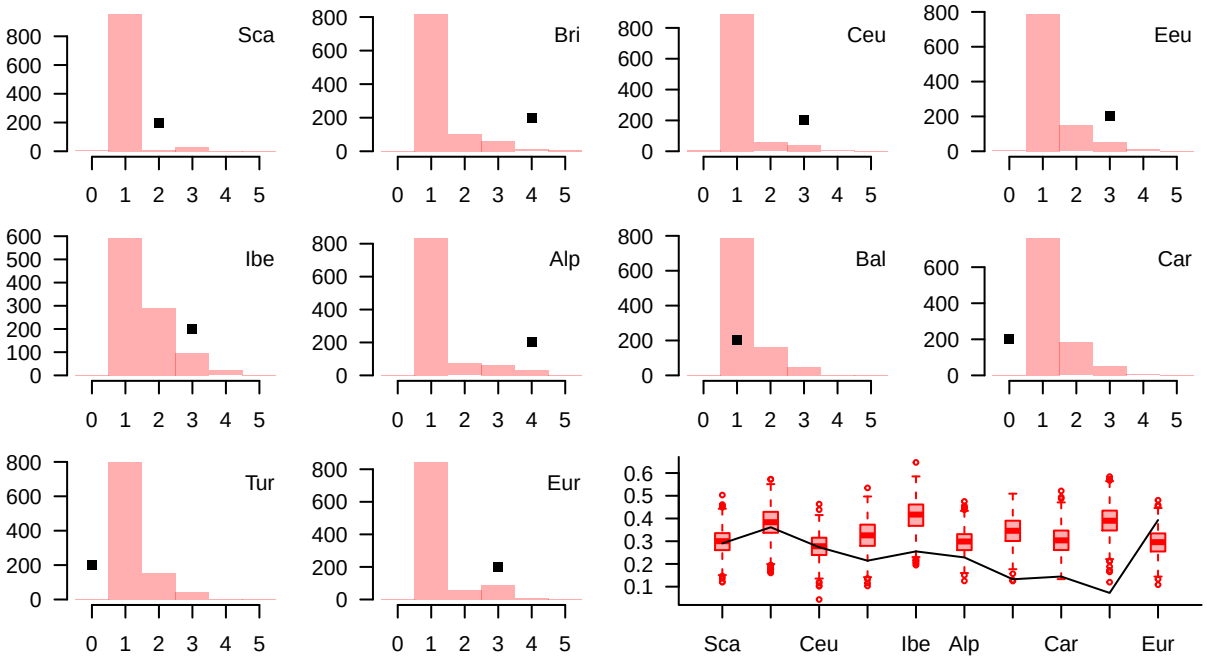

Figure 17: Histograms of order of best autoregressive process fits by region for the BHM-reconstruction ensemble. Panel on bottom right additionally shows boxplots of forced AR(1)-fits. Dots in the histograms and black line in the boxplot panel are for the regional CCLM-simulation output.

Please note, that Luterbacher et al. (2016) assume the temporal autocorrelation of the grid-point data to follow an AR(1)-process. However, this does not necessarily imply that regional averages also follow such a process (compare also Nilsen et al., 2018).

The boxplots in the last panel of Fig 17 suggests that, considering forced AR(1)-fits, the simulation is often similar to the reconstruction series especially for regions in north-western and central Europe and the full domain. Differences appear to be larger in the South-East of Europe, where the simulation gives small AR(1)-fits compared to the majority of reconstruction-ensemble-members. However, I again have to emphasize that there is no proxy-data from this region entering the reconstruction.

The AR-results fit the general assessment of the time-series properties, which shows generally agreement between the simulation and the ensemble reconstruction range. They also agree with the pattern that both data sources agree less in the South-East of Europe.

4 Comparison of the proxies with the simulation grid-points

Another means of assessing simulations and paleo-observations is the comparison of grid-point data, pseudo-proxies, or forward-modelled virtual-proxies from the simulation to the orginal proxy-series. Such an approach could consider all the above analyses plus additional detection and attribution approaches (compare, e.g., PAGES 2k-PMIP3 group, 2015). Although this is a worthwhile enterprise it is a separate document to be written. In the following I only show a short comparison of the original proxies to the nearest simulation grid-point series and the principal components.

4.1 Normalized nearest CCLM-point series vs Euro2K-proxies

Fig 18 shows 47-point Hamming filtered versions of the normalized time-series for the original selection of European proxies (compare PAGES 2k Consortium, 2013; Luterbacher et al., 2016) but excluding the Central European area average data. I compare them with the equivalently processed closest grid-point series from the simulation and also show the correlations between the series for unsmoothed and smoothed versions. The proxy series are from PAGES 2k Consortium (2013, and their references) Torneträsk, Jämtland, Northern Scandinavia, greater Tatra region, Carpathian, Austrian Alps, Swiss Alps, French Alps, Pyrenees, and Albania.

As expected, series do not generally agree between simulations and reconstructions. Correlations are often negligible either for unsmoothed or smoothed data and occasionally for both. Among the proxies, Luterbacher et al. (2016) excluded the data from the Tatra and Albania due to lacking summer temperature signals. Interestingly the Tatra data is the only series notably negatively correlated with the simulation data whereas the data from Albania has some correlation with the smoothed simulation data. However the proxy shows much more variability than the closest simulation grid-point.

Correlations for smoothed data are largest for the Swiss Alps but they are also prominent for the Pyrenees, the French Alps, the Austrian Alps, and Torneträsk. The Northern Scandinavia data, the Jämtland series, and the Carpathian data do not show relevant correlations with the smoothed simulation data although there appear to be some similarities visually. The lack of correlations is mainly due to their opposite evolution in other periods.

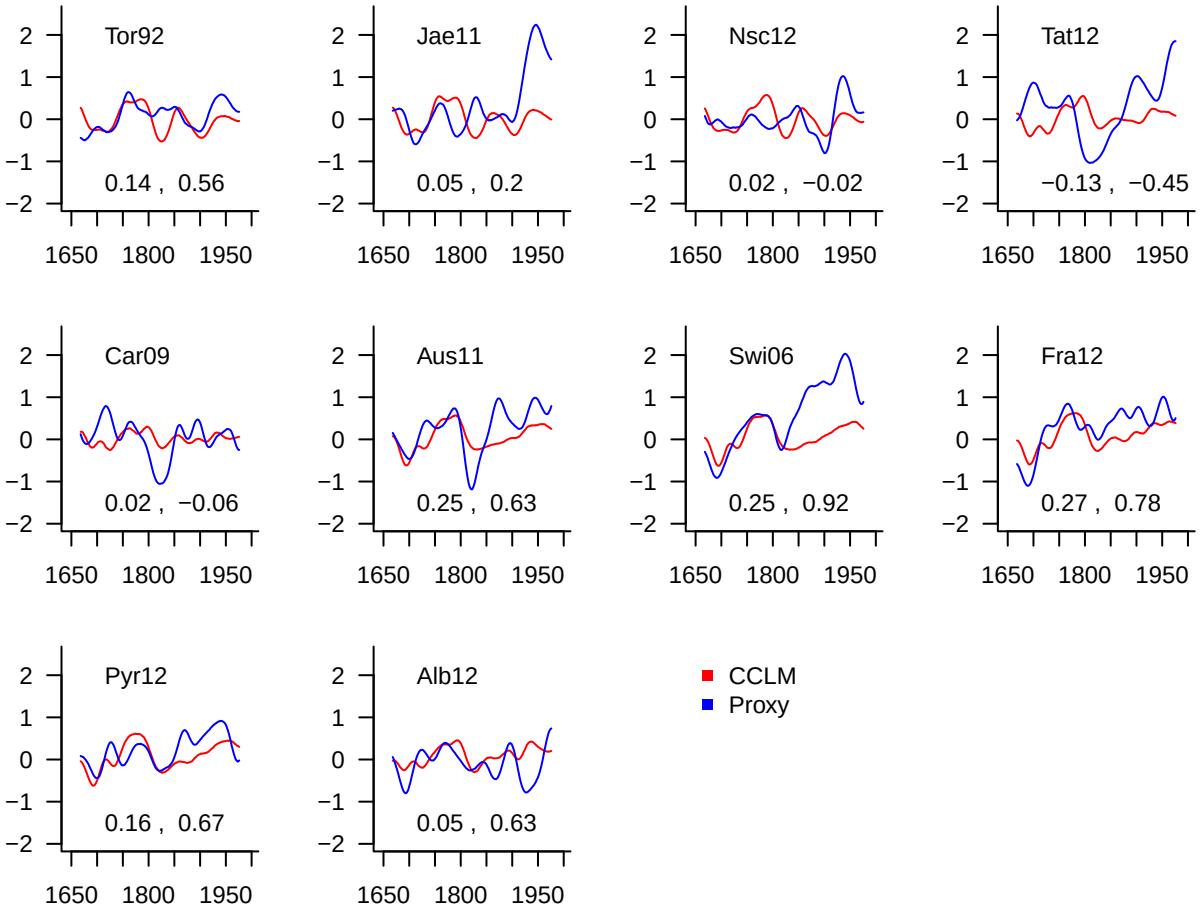

Figure 18: Comparison of the normalized proxy series with the closest simulation-grid-point. Series are 47-point Hamming filtered. Numbers are correlations for the unsmoothed and smoothed data. Labels are from PAGES 2k Consortium (2013): Tor92, Torneträsk, Sweden, Jae11, Jämtland, Sweden, Nsc12, Northern Scandinavia, Tat12, greater Tatra region, Slovakia, Car09, Carpathian, Romania, Aus11, Alps, Austria, Swi06, Alps, Switzerland, Fra12, Alps, France, Pyr12, Pyrenees, Spain, Alb12, Albania. y-axes are non-dimensional. x-axes are Years CE.

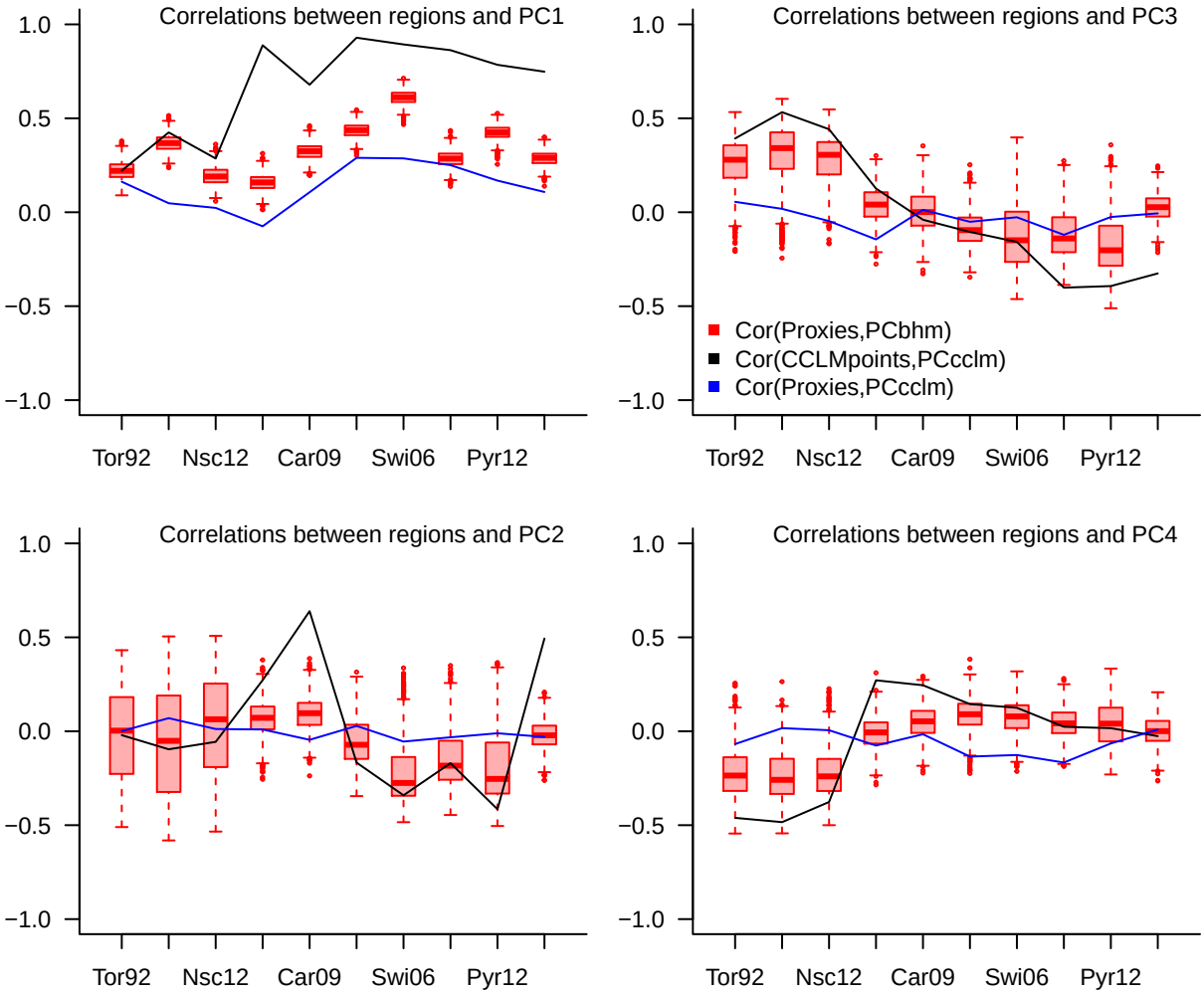

Figure 19: Boxplots: Comparison of correlation coefficients between the reconstruction PCs (PCbhm) and the proxy-series (Proxies). Blue line: Comparison of correlation coefficients between simulation grid points (CCLMpoints) and simulation PCs (PCcclm). Black line: correlation coefficients between proxies and simulation PCs.

4.2 Proxies and PCA

Fig 19 relates the proxies to the reconstruction principal component series, and the closest simulation grid point data to the simulation principal component series. It also adds the correlations between the proxies and the simulation principal component series for information's sake.

Interestingly, the pattern of correlations is similar in the simulation and the reconstruction for all PCs. Even the cross-data-source correlation pattern looks similar for PC1 though correlations are very weak in this case.

Correlations are positive with PC1. Grid-point correlations with PC1 can be very strong in the simulation for grid-points outside of Scandinavia but correlations are more moderate between the original proxies and the reconstruction PC1.

Correlations are predominantly likely negative or about zero for PC2, but the Carpathian and Albania simulation grid-points correlate strongly with this PC. There is a pattern from more likely positive correlations in Scandinavia to more likely negative correlations in more southern regions for PC3. Scandinavia is likely to correlate negatively with PC4, but other regional correlations are about zero or slightly positive. Generally, correlations can be large in the simulation and can be non-negligible for the reconstruction.

The results suggest again that the reconstruction and the simulation show similar spatial interrelations between the locations. On the other hand, there appears to be little to no agreement between the original proxies and the simulated grid-point series.

5 Summary

This report provides simple additional comparisons of the Luterbacher et al. (2016) Euro 2k spatial field reconstruction ensemble with output from a regional climate simulation. Specifically, I use data from a regional simulation with the CCLM model (for the model see Rockel et al., 2008; for the simulation, e.g. Bierstedt et al., 2016).

Reconstruction ensemble and simulation do not generally agree on the evolution over time. Differences in trends and changes in variability are especially noteworthy. Some regions agree better than others.

If I consider the reconstructions as predictions of the simulated temperature evolution, the ensemble generally lacks skill compared to a no-change-reference. Measures of consistency are ambiguous but it is not possible to describe the data sets as climatologically inconsistent.

Similarly, it is not possible to describe time-series properties like spectra, Hurst-exponents, or autoregressive orders as generally different between both data sets. Nevertheless, the simulation data regularly give higher autoregressive orders than the reconstruction data, which may relate to the reconstruction methods.

This lack of disagreement is encouraging. Even more encouraging is the apparent agreement in spatial covariations between the regional series as found in a principal component analysis, which even translates to their evolution over time. The similarity in relations also extends to comparisons of the original proxies or equivalent simulation grid-points with the PC time series.

In my analyses, I take advantage of the ensemble-character of the Luterbacher et al. (2016) Bayesian Hierarchichal Modelling Euro 2k field reconstruction. This provides, on the one hand, a, possibly incomplete, estimate of the uncertainty of the reconstruction. More importantly, it also gives a natural confidence limit for the comparison of the simulation data with the reconstructed estimates of past summer temperature changes in Europe and the sub-domains I use.

The use of the full ensemble highlights the benefits of ensemble approaches or more general of providing credible uncertainty estimates for reconstructions. Uncertainty estimates for the original proxies would also be helpful for further comparison studies. The document also adds a few additional analyses to the suite of analyses suggested by the PAGES 2k-PMIP3 group (2015).

One interesting feature of most analyses is that simulation and reconstruction ensemble are least similar in the South-East of Europe. On the one hand, the reconstruction does not include any proxy-information from this region. On the other hand, this is the region where the influences of the large scale weather and climate situation over the North Atlantic and western Europe are least important.

The apparent occasional agreement in some regional time-series, trends, and variability-series warrants a short additional discussion. While this is encouraging I cannot rule out that this agreement is coincidental due to different effects in proxies and simulation. That is, reconstruction and simulation agree due to the wrong reasons. Periods of agreement appear visually to relate to reconstructed changes of past climate forcings (e.g., Schmidt et al., 2011; Fernández-Donado et al., 2013; Luterbacher et al., 2016; PAGES 2k-PMIP3 group, 2015). Numerous studies document the influence of volcanic eruptions on surface temperature in Europe, but evidence is weaker for a temperature-effect of solar variability. In the simulation, potential relations between solar forcing variations and surface temperature have to be due to a direct effect because of the vertical extent of the simulation setup and the implementation of forcing variations. That is, there is unlikely a complex chain of dynamic interactions leading to regional temperature variability. See Shindell et al. (2003) or, e.g., also Anet et al. (2014) for studies of the influence of solar forcing variations on the climate. Put clearly, if there is an influence of the solar variations on the near surface air temperature in the simulation it is not due to a credible mechanism. This also accounts for the possibility that the lateral forcing by the global simulation imprints this relation on the regional simulation.

It is tempting to intepret the reconstruction similarly. However, the proxies generally react to more than one environmental influence. Therefore, solar signals in the proxy may also be due to factors like precipitation, dryness, cloud cover, or circulation despite a general temperature sensitivity. The proxy may not represent a direct temperature influence and thus a solar effect on temperature but a signal of circulation variability due to variations in solar activity.

This short summary highlights that best progress in our understanding of past climate changes may come from better constraining past climate forcing variability, better understanding of proxy-environment-relations, better proxy- and reconstruction-uncertainty estimates, and better understanding of forcing influences on simulated regional climate. While the agreement in certain climatic and statistical properties between simulations and reconstructions is encouraging, a lot of work remains to be done to be confident about past climate changes and their origins.

6 Data and code availability

The simulation output for temperature is available at Figshare [PRIME2 (2018); doi.org/10.6084/m9.figshare.5952025]. The reconstruction data is available from https://www.ncdc.noaa.gov/

paleo-search/study/19600 though the file may have to be saved differently to use it in the analyses. The proxy-series are available from https://www.nature.com/articles/ngeo1797. Long instrumental and regionally representative series can be obtained from http://berkeleyearth.org/data/ to extend the present analyses.

7 External code

I used the Climate Data Operators (CDO) of the Max Planck Institute for Meteorology to manipulate netcdf-files. Otherwise, I used R (R Core Team, 2018a) mostly within the environment of Rstudio (RStudio Team, 2016). The following packages helped in this project: zoo (Zeileis and Grothendieck, 2005), astsa (Stoffer, 2017), gtools (Warnes et al., 2018), dplR (Bunn, 2008), ncdf (Pierce, 2015), pastecs (Grosjean and Ibanez, 2018), gdata (Warnes et al., 2017), corrplot (Wei and Simko, 2017), oce (Kelley and Richards, 2018), roll (Foster, 2018), knitr (Xie, 2018), kableExtra (Zhu, 2018), grDevices (R Core Team, 2018b), fields (Nychka et al., 2017), ensembleBMA (Fraley et al., 2018), psd (Barbour and Parker, 2014), pracma (Borchers, 2018), tseries (Trapletti and Hornik, 2018), forecast (Hyndman and Khandakar, 2008), and Rodriguez-Sanchez (2017; Rodriguez-Sanchez, 2017). The Hamming filter code follows a script provided by Martin Widmann.

8 Competing interests

I am not aware of any circumstances that might be seen as competing interests.

9 Acknowledgements

This work was mostly done while I received funding within PRIME 2 and PALMOD (www.palmod.de). Sebastian Wagner provided the CCLM model data. This report contributes to the PAGES 2k Network especially its PALEOLINK project. Comments by Johannes Werner helped to improve the manuscript.

10 Appendix: Supplementary Figures

The following simply collects a number of additional Figures without comment.

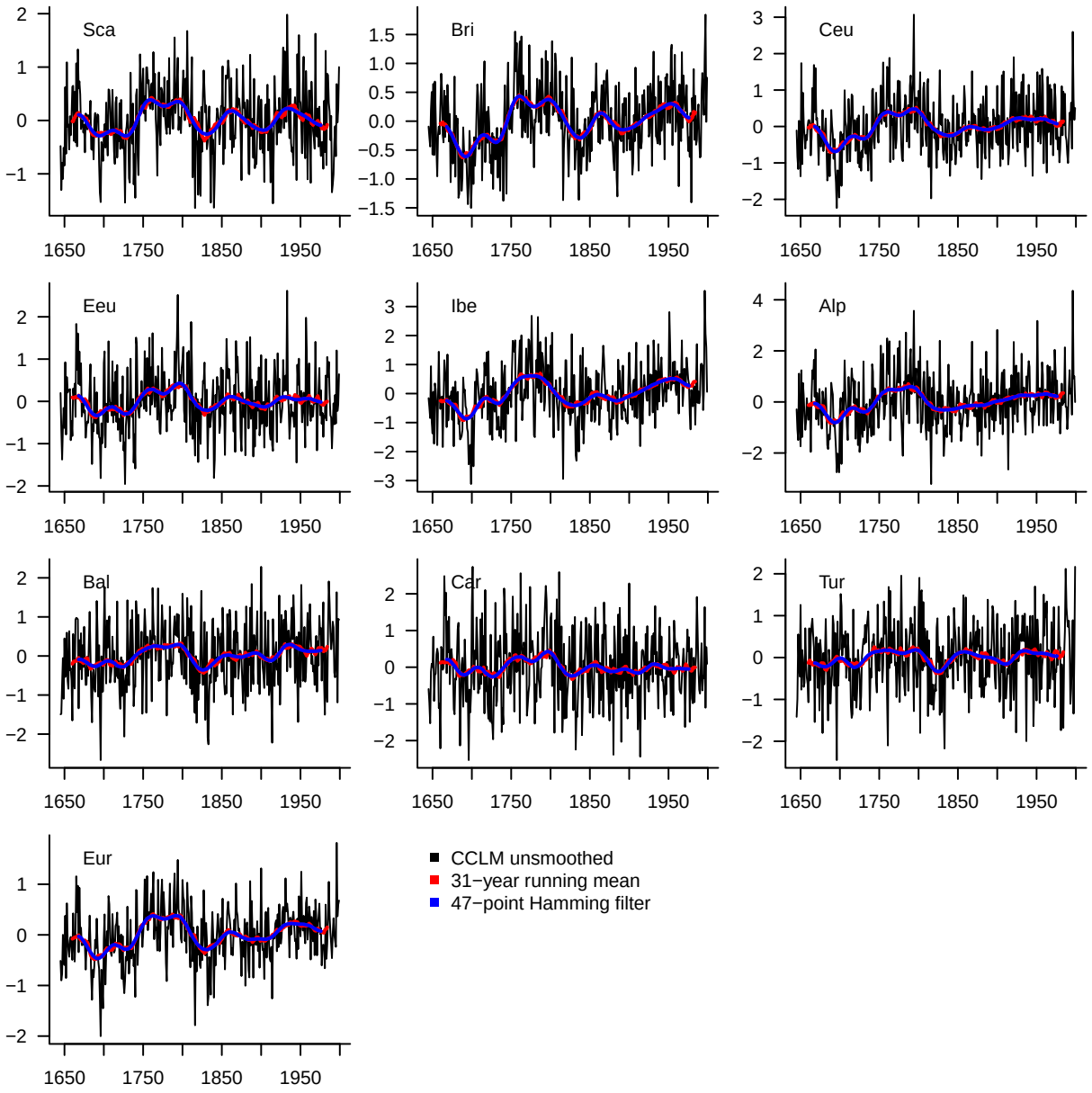

Figure 20: CCLM-simulation-data: Temperature anomalies for regional means relative to the climatology for the period 1645-1850. Black: annual resolution. Red: 31-year running mean. Blue: 31-year-equivalent 47-point Hamming-Filter. Sca: Scandinavia, Bri: Britain and Ireland, Ceu: Central Europe, Eeu: Eastern Europe, Ibe: Iberian Peninsula, Alp: Alps, Bal: Balkan Peninsula, Car: Carpathian region, Tur: Turkey, Eur: full European region.

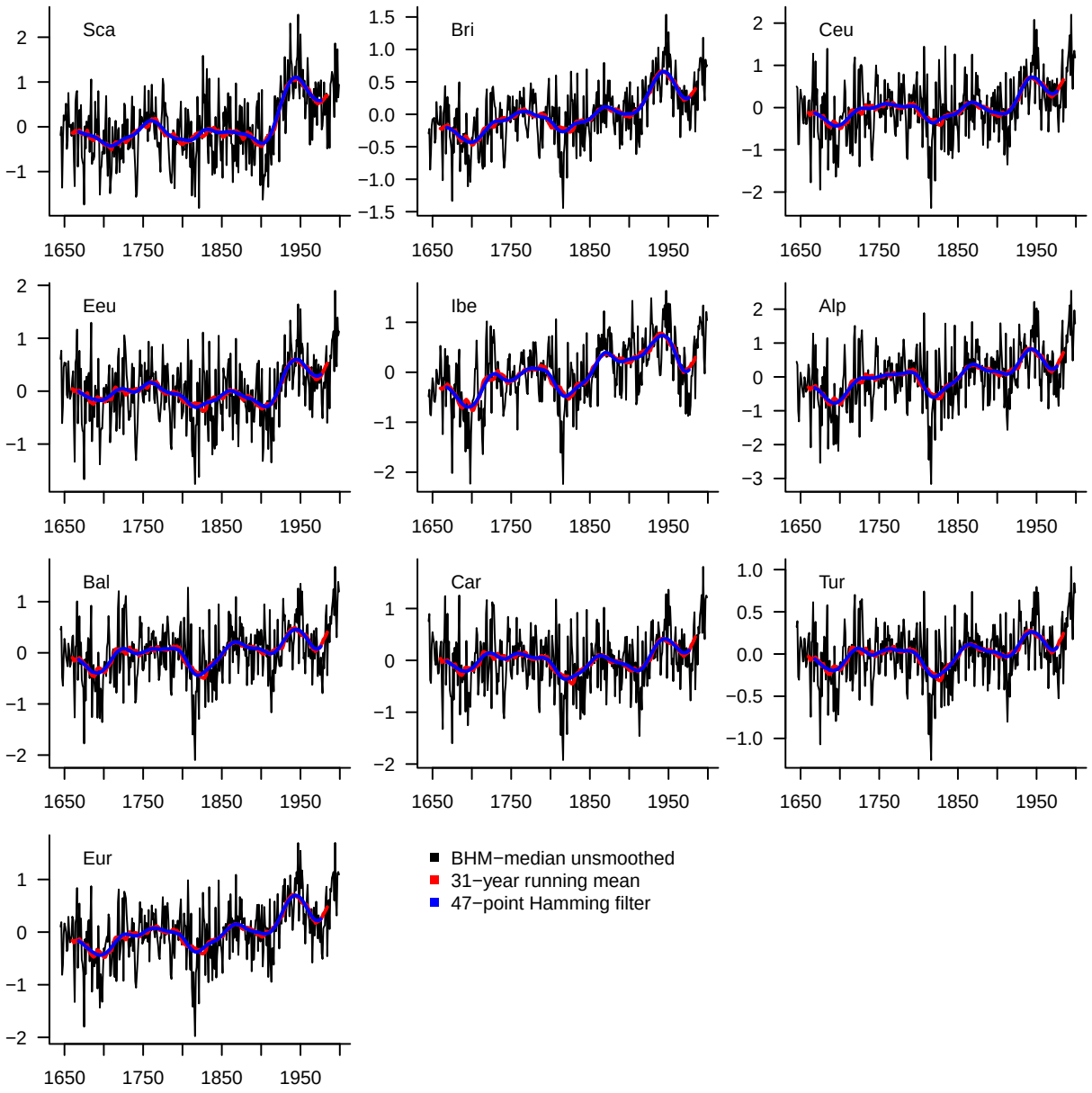

Figure 21: BHM-reconstruction-data, median: Temperature anomalies for regional means relative to the climatology for the period 1645-1850. Black: annual resolution. Red: 31-year running mean. Blue: 31-year-equivalent 47-point Hamming-Filter. Sca: Scandinavia, Bri: Britain and Ireland, Ceu: Central Europe, Eeu: Eastern Europe, Ibe: Iberian Peninsula, Alp: Alps, Bal: Balkan Peninsula, Car: Carpathian region, Tur: Turkey, Eur: full European region.

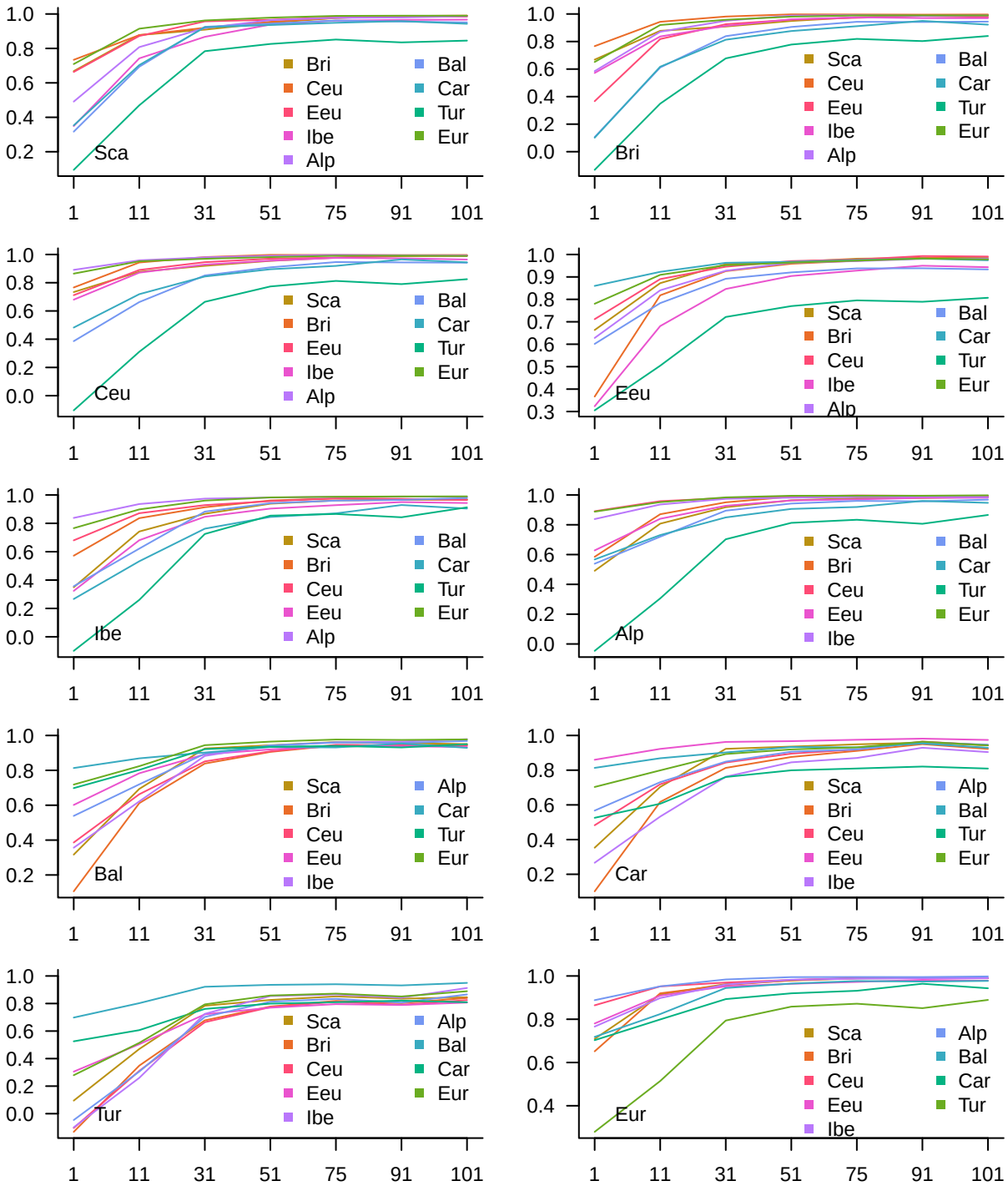

Figure 22: Summary of interregional correlations of smoothed simulation data series. Panels show how interregional correlation coefficients change between smoothing window-lengths. x-axis are smoothing window-sizes of 1, 11, 31, 51, 71, 91, and 101 years. y-axes are correlation coefficients.

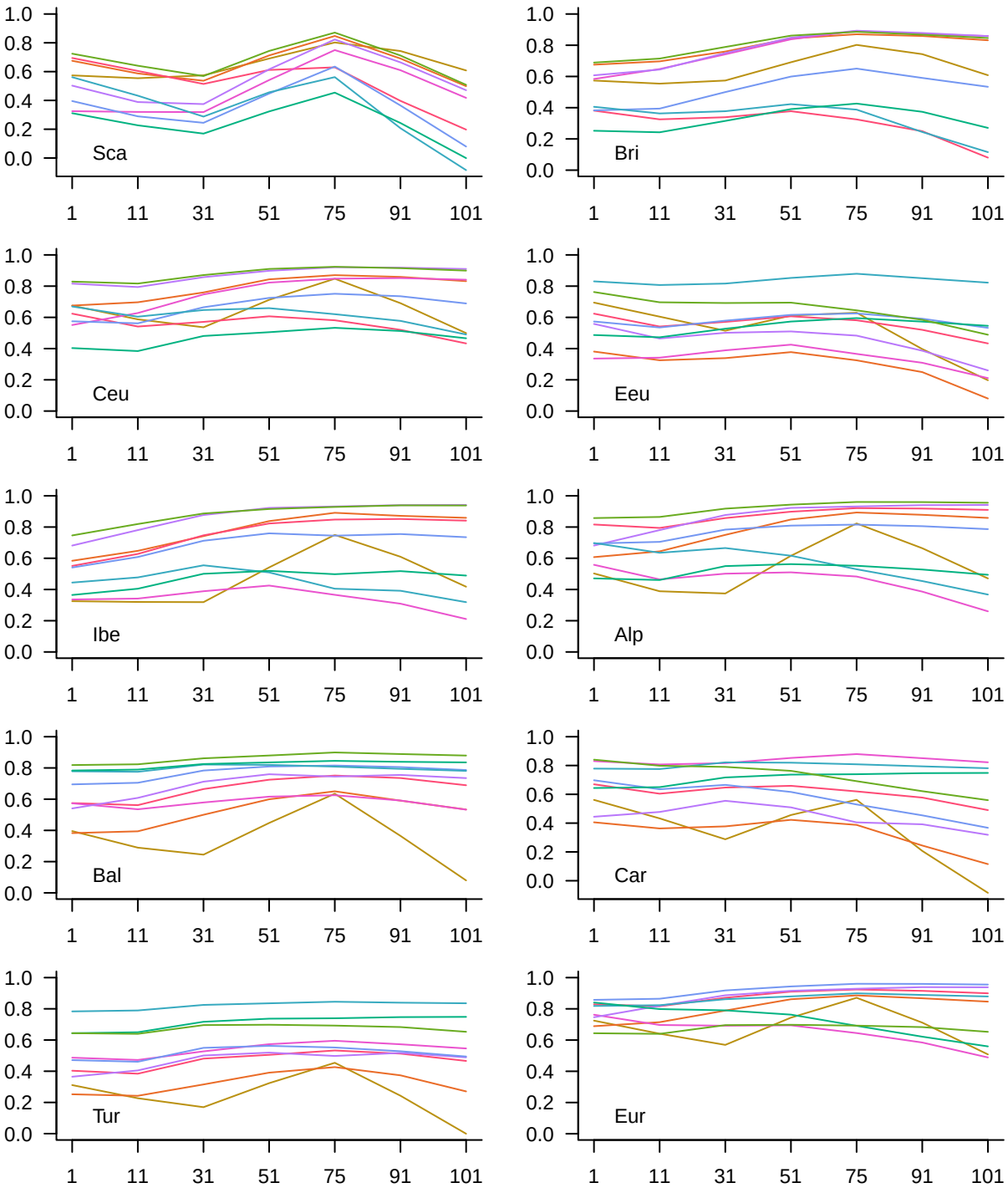

Figure 23: Summary of median interregional correlations of smoothed reconstruction series. Panels show how interregional correlation coefficients change between smoothing window-lengths. x-axis are smoothing window-sizes of 1, 11, 31, 51, 71, 91, and 101 years. y-axes are correlation coefficients.

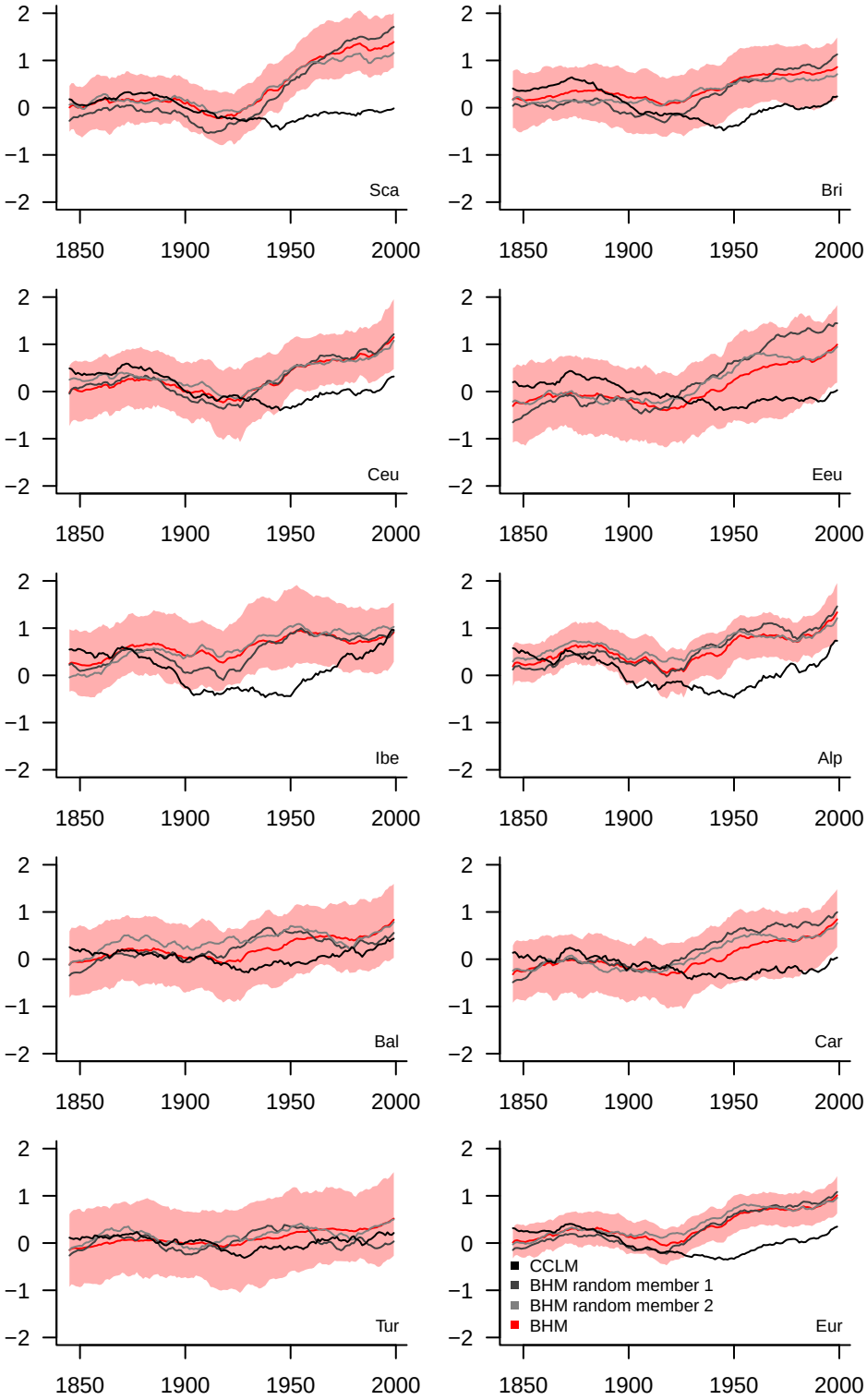

Figure 24: Comparison of 201-year moving linear trend fits for the regional CCLM-simulation output, the median of the smoothed BHM-reconstruction ensemble, and two random members of the ensemble.

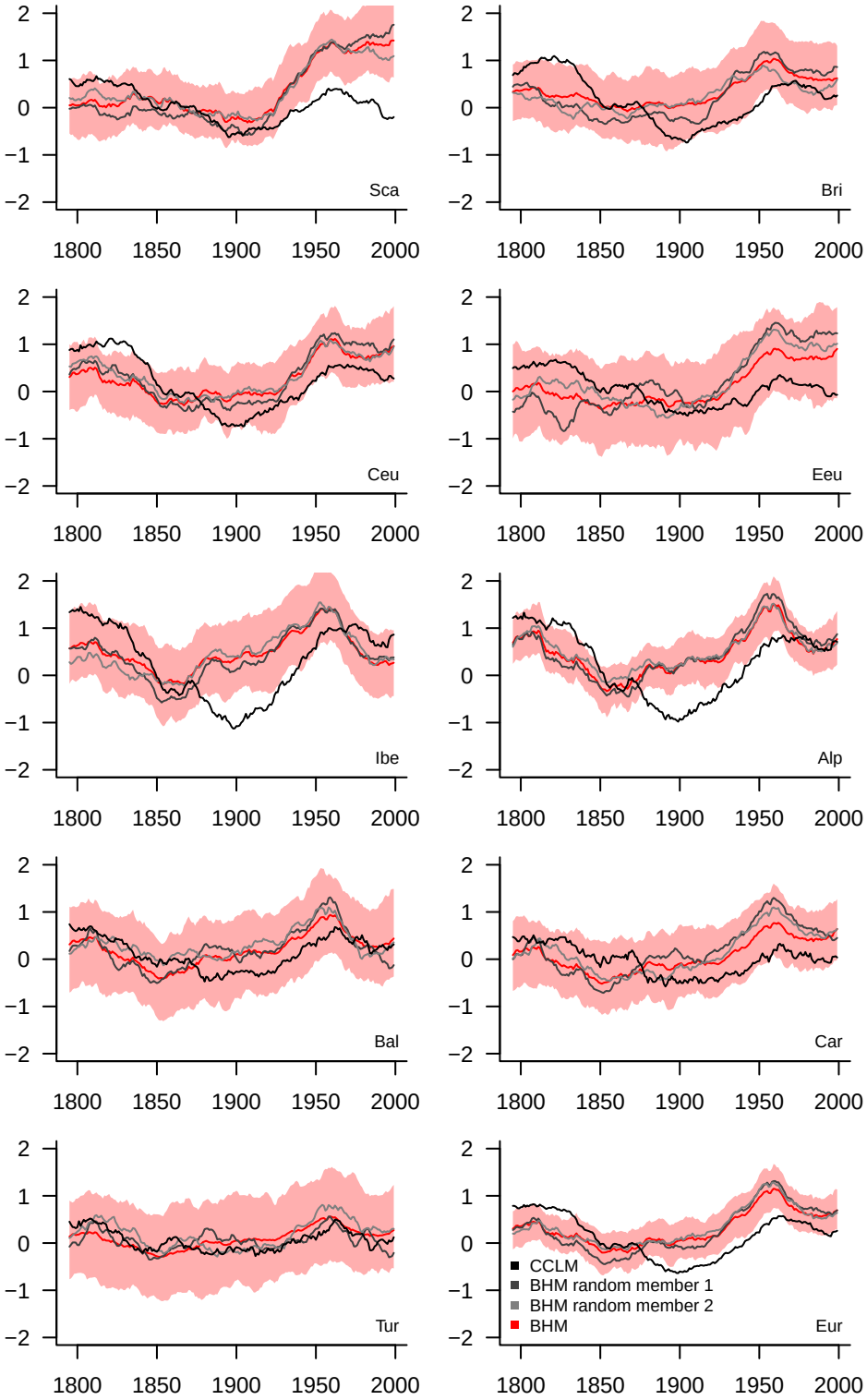

Figure 25: Comparison of 151-year moving linear trend fits for the regional CCLM-simulation output, the median of the smoothed BHM-reconstruction ensemble, and two random members of the ensemble.

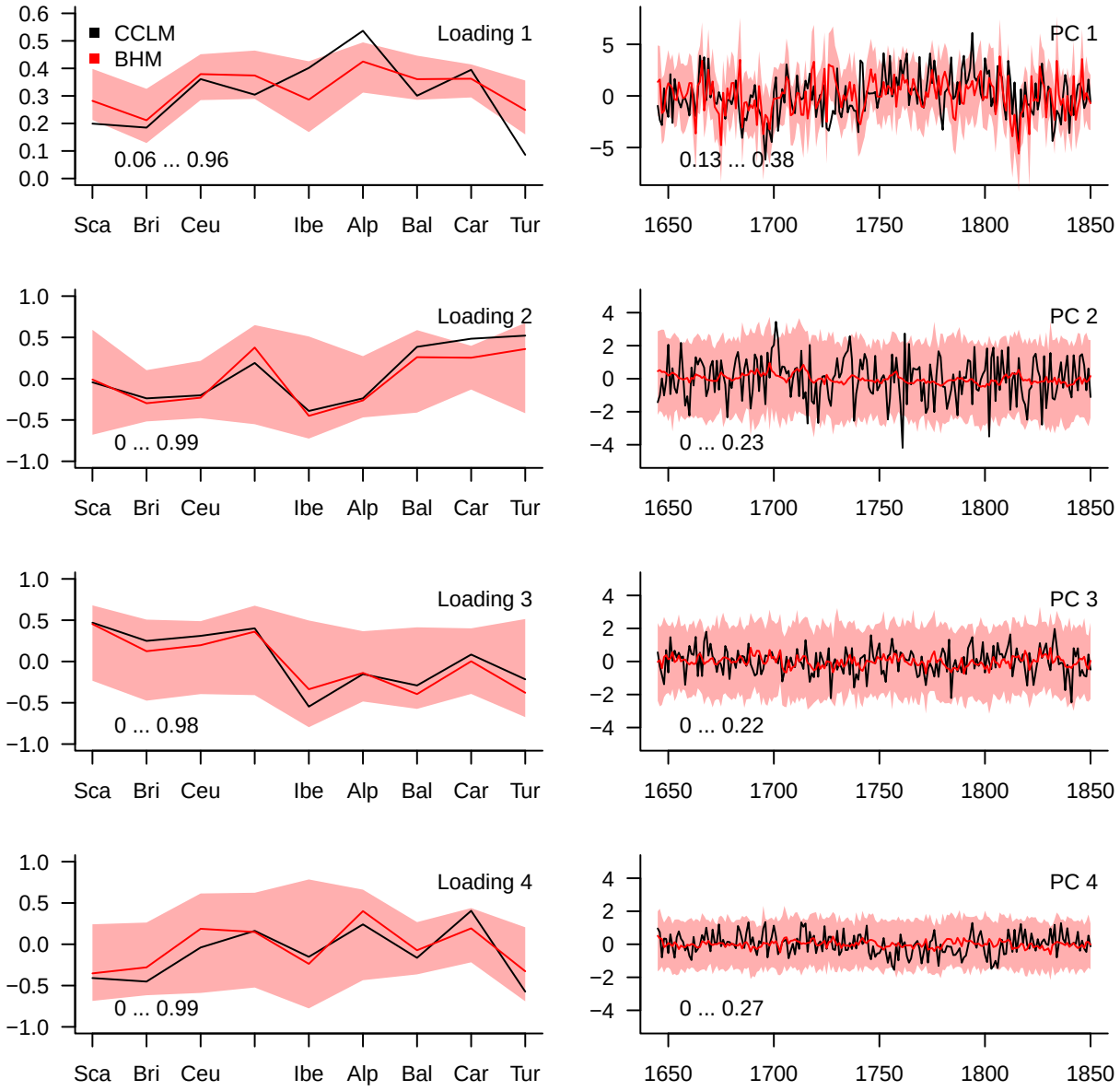

Figure 26: Principal component analysis over the regional series for principal components 1 to 4 from top to bottom. Left: Loading. Right: Interannual time series. Shading is the full range of the reconstruction loadings and the smoothed reconstruction time-series. The red line is the median. The black line is for the simulation output. Numbers in the bottom left corner are the range of correlations between the simulation-PC and the reconstruction ensemble PCs. y-axes are non-dimensional values. x-axes for the loadings are the regions, and years CE for the time-series.

References

Anderson, J. L.: A Method for Producing and Evaluating Probabilistic Forecasts from Ensemble Model Integrations, J. Climate, 9, 1518–1530, https://doi.org/10.1175/1520-0442(1996)009\%3C1518:amfpae\%3E2.0.co;2, 1996.

Anet, J. G., Muthers, S., Rozanov, E. V., Raible, C. C., Stenke, A., Shapiro, A. I., Brönnimann, S., Arfeuille, F., Brugnara, Y., Beer, J., Steinhilber, F., Schmutz, W., and Peter, T.: Impact of solar versus volcanic activity variations on tropospheric temperatures and precipitation during the Dalton Minimum, Climate of the Past, 10, 921–938, https://doi.org/10.5194/cp-10-921-2014, 2014.

Annan, J. D. and Hargreaves, J. C.: Reliability of the CMIP3 ensemble, Geophysical Research Letters, 37, https://doi.org/10.1029/2009GL041994, 2010.

Barbour, A. J. and Parker, R. L.: psd: Adaptive, sine multitaper power spectral density estimation for R, Computers & Geosciences, 63, 1–8, https://doi.org/10.1016/j.cageo.2013.09.015, 2014.

Bierstedt, S. E., Hünicke, B., Zorita, E., Wagner, S., and Gómez-Navarro, J. J.: Variability of daily winter wind speed distribution over Northern Europe during the past millennium in regional and global climate simulations, Climate of the Past, 12, 317–338, https://doi.org/10.5194/cp-12-317-2016, 2016.

Borchers, H. W.: pracma: Practical Numerical Math Functions, URL https://CRAN.R-project.org/package=pracma, r package version 2.1.4, 2018.

Bunde, A., Buntgen, U., Ludescher, J., Luterbacher, J., and von Storch, H.: Is there memory in precipitation?, Nature Clim. Change, 3, 174–175, https://doi.org/10.1038/nclimate1830, 2013.

Bunn, A. G.: A dendrochronology program library in R (dplR), Dendrochronologia, 26, 115–124, https://doi.org/10.1016/j.dendro.2008.01.002, URL http://dx.doi.org/10.1016/j.dendro.2008.01.002, 2008.

Deser, C., Phillips, A., Bourdette, V., and Teng, H.: Uncertainty in climate change projections: the role of internal variability, Climate Dynamics, 38, 527–546, https://doi.org/10.1007/s00382-010-0977-x, 2012.

Dobrovolný, P., Rybníček, M., Büntgen, U., Trnka, M., Brázdil, R., Stachoň, Z., Prokop, O., and Kolář, T.: Recent growth coherence in long-term oak (Quercus spp.) ring width chronologies in the Czech Republic, Climate Research, 70, 133–141, https://doi.org/10.3354/cr01402, URL http://www.int-res.com/abstracts/cr/v70/n2-3/p133-141/, 2016.

Evans, M. N., Tolwinski-Ward, S. E., Thompson, D. M., and Anchukaitis, K. J.: Applications of proxy system modeling in high resolution paleoclimatology, Quaternary Science Reviews, 76, 16–28, https://doi.org/10.1016/j.quascirev.2013.05.024, 2013.

Fernández-Donado, L., González-Rouco, J. F., Raible, C. C., Ammann, C. M., Barriopedro, D., Garcıa-Bustamante, E., Jungclaus, J. H., Lorenz, S. J., Luterbacher, J., Phipps, S. J., Servonnat, J., Swingedouw, D., Tett, S. F. B., Wagner, S., Yiou, P., and Zorita, E.: Large-scale temperature response to external forcing in simulations and reconstructions of the last millennium, Climate of the Past, 9, 393–421, https://doi.org/10.5194/cp-9-393-2013, 2013.

Foster, J.: roll: Rolling Statistics, URL https://CRAN.R-project.org/package=roll, r package version 1.1.1, 2018.

Fraley, C., Raftery, A. E., Sloughter, J. M., Gneiting, T., and of Washington., U.: ensembleBMA: Probabilistic Forecasting using Ensembles and Bayesian Model Averaging, URL https://CRAN.R-project.org/package=ensembleBMA, r package version 5.1.5, 2018.

Gómez-Navarro, J. J., Montávez, J. P., Wagner, S., and Zorita, E.: A regional climate palaeosimulation for Europe in the period 1500–1990 – Part 1: Model validation, Climate of the Past, 9, 1667–1682, https://doi.org/10.5194/cp-9-1667-2013, URL http://dx.doi.org/10.5194/cp-9-1667-2013, 2013.

Gómez-Navarro, J. J., Bothe, O., Wagner, S., Zorita, E., Werner, J. P., Luterbacher, J., Raible, C. C., and Montávez, J. P.: A regional climate palaeosimulation for Europe in the period 1500-1990 - Part 2: Shortcomings and strengths of models and reconstructions, Climate of the Past, 11, 1077–1095, https://doi.org/10.5194/cp-11-1077-2015, 2015.

Gómez-Navarro, J. J., Werner, J. P., Wagner, S., Zorita, E., and Luterbacher, J.: Precipitation in the Past Millennium in Europe—Extension to Roman Times, in: Integrated Analysis of Interglacial Climate Dynamics (INTERDYNAMIC), edited by Schulz, M. and Paul, A., pp. 133–139, Springer International Publishing, Cham, https://doi.org/10.1007/978-3-319-00693-2_22, 2015.

Grosjean, P. and Ibanez, F.: pastecs: Package for Analysis of Space-Time Ecological Series, URL https://CRAN.R-project.org/package=pastecs, r package version 1.3.21, 2018.

Hakim, G. J., Emile-Geay, J., Steig, E. J., Noone, D., Anderson, D. M., Tardif, R., Steiger, N., and Perkins, W. A.: The last millennium climate reanalysis project: Framework and first results, Journal of Geophysical Research, 121, 6745–6764, https://doi.org/10.1002/2016JD024751, 2016.

Hamill, T. M.: Interpretation of Rank Histograms for Verifying Ensemble Forecasts, Mon. Wea. Rev., 129, 550–560, https://doi.org/10.1175/1520-0493(2001)129\%3C0550:iorhfv\%3E2.0.co;2, 2001.

Hargreaves, J. C., Annan, J. D., Ohgaito, R., Paul, A., and Abe-Ouchi, A.: Skill and reliability of climate model ensembles at the Last Glacial Maximum and mid-Holocene, Climate of the Past, 9, 811–823, https://doi.org/10.5194/cp-9-811-2013, 2013.

Hyndman, R. J. and Khandakar, Y.: Automatic time series forecasting: the forecast package for R, Journal of Statistical Software, 26, 1–22, URL http://www.jstatsoft.org/article/view/v027i03, 2008.

Jolliffe, I. T. and Primo, C.: Evaluating Rank Histograms Using Decompositions of the Chi-Square Test Statistic, Mon. Wea. Rev., 136, 2133–2139, https://doi.org/10.1175/2007mwr2219.1, 2008.

Jungclaus, J. and Esch, M.: mil0021: MPI-M Earth System Modelling Framework: millennium full forcing experiment using solar forcing of Bard, URL http://cera-www.dkrz.de/WDCC/ui/Compact.jsp?acronym=mil0021, 2009.

Jungclaus, J. H., Lorenz, S. J., Timmreck, C., Reick, C. H., Brovkin, V., Six, K., Segschneider, J., Giorgetta, M. A., Crowley, T. J., Pongratz, J., Krivova, N. A., Vieira, L. E., Solanki, S. K., Klocke, D., Botzet, M., Esch, M., Gayler, V., Haak, H., Raddatz, T. J., Roeckner, E., Schnur, R., Widmann, H., Claussen, M., Stevens, B., and Marotzke, J.: Climate and carbon-cycle variability over the last millennium, Climate of the Past, 6, 723–737, https://doi.org/10.5194/cp-6-723-2010, 2010.

Kelley, D. and Richards, C.: oce: Analysis of Oceanographic Data, URL https://CRAN.R-project.org/package=oce, r package version 0.9-23, 2018.

Ludwig, P., Gómez-Navarro, J. J., Pinto, J. G., Raible, C. C., Wagner, S., and Zorita, E.: Perspectives of regional paleoclimate modeling, Annals of the New York Academy of Sciences, https://doi.org/10.1111/nyas.13865, 2018.

Luterbacher, J., Werner, J. P., Smerdon, J. E., Fernández-Donado, L., González-Rouco, F. J., Barriopedro, D., Ljungqvist, F. C., Büntgen, U., Zorita, E., Wagner, S., Esper, J., McCarroll, D., Toreti, A., Frank, D., Jungclaus, J. H., Barriendos, M., Bertolin, C., Bothe, O., Brázdil, R., Camuffo, D., Dobrovolný, P., Gagen, M., García-Bustamante, E., Ge, Q., Gómez-Navarro, J. J., Guiot, J., Hao, Z., Hegerl, G. C., Holmgren, K., Klimenko, V. V., Martín-Chivelet, J., Pfister, C., Roberts, N., Schindler, A., Schurer, A., Solomina, O., von Gunten, L., Wahl, E., Wanner, H., Wetter, O., Xoplaki, E., Yuan, N., Zanchettin, D., Zhang, H., and Zerefos, C.: European summer temperatures since Roman times, Environmental Research Letters, 11, 24 001, https://doi.org/10.1088/1748-9326/11/2/024001, 2016.

Marzban, C., Wang, R., Kong, F., and Leyton, S.: On the Effect of Correlations on Rank Histograms: Reliability of Temperature and Wind Speed Forecasts from Finescale Ensemble Reforecasts, Mon. Wea. Rev., 139, 295–310, https://doi.org/10.1175/2010mwr3129.1, 2010.

Nilsen, T., Werner, J. P., Divine, D. V., and Rypdal, M.: Assessing the performance of the BARCAST climate field reconstruction technique for a climate with long-range memory, Climate of the Past, 14, 947–967, https://doi.org/10.5194/cp-14-947-2018, 2018.

Nychka, D., Furrer, R., Paige, J., and Sain, S.: fields: Tools for spatial data, https://doi.org/10.5065/D6W957CT, URL www.image.ucar.edu/~nychka/Fields, r package version 9.6, 2017.

PAGES 2k Consortium: Continental-scale temperature variability during the past two millennia, Nature Geoscience, 6, 339–346, https://doi.org/10.1038/ngeo1797, 2013.

PAGES 2k-PMIP3 group: Continental-scale temperature variability in PMIP3 simulations and PAGES 2k regional temperature reconstructions over the past millennium, Climate of the Past, 11, 1673–1699, https://doi.org/10.5194/cp-11-1673-2015, 2015.

PAGES Hydro2k Consortium: Comparing proxy and model estimates of hydroclimate variability and change over the Common Era, Climate of the Past, 13, 1851–1900, https://doi.org/10.5194/cp-13-1851-2017, 2017.

Pierce, D.: ncdf: Interface to Unidata netCDF Data Files, URL https://CRAN.R-project.org/package=ncdf, r package version 1.6.9, 2015.

PRIME2: Precipitation and Temperature from a Regional Climate Model simulation with CCLM for Europe over the period 1645-1999CE, https://doi.org/10.6084/m9.figshare.5952025, 2018.

R Core Team: R: A Language and Environment for Statistical Computing, R Foundation for Statistical Computing, Vienna, Austria, URL https://www.R-project.org/, 2018a.

R Core Team: R: A Language and Environment for Statistical Computing, R Foundation for Statistical Computing, Vienna, Austria, URL https://www.R-project.org/, 2018b.

Rockel, B., Will, A., and Hense, A.: The Regional Climate Model COSMO-CLM (CCLM), Meteorologische Zeitschrift, 17, 347–348, https://doi.org/10.1127/0941-2948/2008/0309, 2008.

Rodriguez-Sanchez, F.: grateful: Facilitate Citation of R Packages, URL https://github.com/Pakillo/grateful, r package version 0.0.1, 2017.

RStudio Team: RStudio: Integrated Development Environment for R, RStudio, Inc., Boston, MA, URL http://www.rstudio.com/, 2016.

Schmidt, G. A., Jungclaus, J. H., Ammann, C. M., Bard, E., Braconnot, P., Crowley, T. J., Delaygue, G., Joos, F., Krivova, N. A., Muscheler, R., Otto-Bliesner, B. L., Pongratz, J., Shindell, D. T., Solanki, S. K., Steinhilber, F., and Vieira, L. E. A.: Climate forcing reconstructions for use in PMIP simulations of the last millennium (v1.0), Geoscientific Model Development, 4, 33–45, https://doi.org/10.5194/gmd-4-33-2011, 2011.

Shindell, D. T., Schmidt, G. A., Miller, R. L., and Mann, M. E.: Volcanic and Solar Forcing of Climate Change during the Preindustrial Era, Journal of Climate, 16, 4094–4107, https://doi.org/10.1175/1520-0442(2003)016<4094:VASFOC>2.0.CO;2, 2003.

Stoffer, D.: astsa: Applied Statistical Time Series Analysis, URL https://CRAN.R-project.org/package=astsa, r package version 1.8, 2017.

Tolwinski-Ward, S. E., Evans, M. N., Hughes, M. K., and Anchukaitis, K. J.: An efficient forward model of the climate controls on interannual variation in tree-ring width, Climate Dynamics, 36, 2419–2439, https://doi.org/10.1007/s00382-010-0945-5, 2011.

Trapletti, A. and Hornik, K.: tseries: Time Series Analysis and Computational Finance, URL https://CRAN.R-project.org/package=tseries, r package version 0.10-45., 2018.

Warnes, G. R., Bolker, B., Gorjanc, G., Grothendieck, G., Korosec, A., Lumley, T., MacQueen, D., Magnusson, A., Rogers, J., and others: gdata: Various R Programming Tools for Data Manipulation, URL https://CRAN.R-project.org/package=gdata, r package version 2.18.0, 2017.

Warnes, G. R., Bolker, B., and Lumley, T.: gtools: Various R Programming Tools, URL https://CRAN.R-project.org/package=gtools, r package version 3.8.1, 2018.

Wei, T. and Simko, V.: R package "corrplot": Visualization of a Correlation Matrix, URL https://github.com/taiyun/corrplot, (Version 0.84), 2017.

Weron, R.: Estimating long-range dependence: finite sample properties and confidence intervals, Physica A: Statistical Mechanics and its Applications, 312, 285–299, https://doi.org/10.1016/S0378-4371(02)00961-5, 2002.

Xie, Y.: knitr: A General-Purpose Package for Dynamic Report Generation in R, URL https://yihui.name/knitr/, r package version 1.20, 2018.

Zeileis, A. and Grothendieck, G.: zoo: S3 Infrastructure for Regular and Irregular Time Series, Journal of Statistical Software, 14, 1–27, https://doi.org/10.18637/jss.v014.i06, 2005.

Zhu, H.: kableExtra: Construct Complex Table with 'kable' and Pipe Syntax, URL https://CRAN.R-project.org/package=kableExtra, r package version 0.9.0, 2018.